A Mechanism of Resistance and Mode of Action for Drugs Against *Plasmodium falciparum*

Anne Elizabeth Purfield

A dissertation submitted to the faculty of the University of North Carolina at Chapel Hill in partial fulfillment of the requirements for the degree of Doctor of Philosophy in the Department of Microbiology and Immunology.

Chapel Hill
2007

Approved By:

Steven R. Meshnick

Edward Collins

Peter Gilligan

Marcia Hobbs

Richard R. Tidwell

ABSTRACT

Anne Elizabeth Purfield: A Mechanism of Resistance and Mode of Action for Drugs Against *Plasmodium falciparum*
(Under the direction of Steven R. Meshnick, M.D., Ph.D.)

The need for new drugs to control widespread malaria caused by *Plasmodium falciparum* is critical. Parasite resistance to currently used drugs is rampant and, in many cases, the drug's mode of action and/or mechanism of resistance is unknown. The three objectives of this dissertation address issues associated with resistance to the currently used antimalarial drugs, in addition to elucidating the mechanism of action of a novel antimalarial compound in development.

First, a real time PCR method was developed to distinguish parasite genotypes associated with mefloquine resistance in vitro. Single nucleotide point mutations in the *Plasmodium falciparum multi-drug resistance-1* (*pfmdr1*) gene are associated with mefloquine resistance in vitro. This method may be applied to clinical malaria samples and used to predict treatment outcome as well as for surveillance of drug resistance.

In addition, the mechanism of action for the novel compound, [2,5-bis(4-amidinophenyl) furan], (DB75) was investigated. DB75, the active metabolite of the oral pro-drug DB289, is a broad spectrum antiparasitic agent with impressive antimalarial activity both in vitro and in vivo. It is currently in development for treatment of falciparum malaria, however the mode of action against falciparum parasites is unknown. Results from ultraviolet confocal microscopy showed DB75 localization exclusively in the nucleus of parasites in culture. Further, microscopy studies using blood smears to distinguish morphologies suggested DB75

has a life stage-specific mechanism. Parasites must be exposed during the ring stage for effective killing. Finally, real time PCR gene expression assays suggested high concentrations of DB75 may alter the expression pattern in a manner consistent with the delay in maturation. However, DB75 did not inhibit or enhance global nuclear transcription or developmental expression of six select genes.

The third objective was to determine potential synergistic interactions of DB75 in combination with current antimalarial drugs to determine a mechanism of action for DB75 and to identify potential partner drugs for use in combination therapy with DB75.

Taken together, this work contributes to the arsenal of tools for surveillance of falciparum malaria drug resistance and partially elucidates a mechanism of action for a novel antimalarial diamidine that may be used for malaria therapy.

ACKNOWLEDGEMENTS

I thank my adviser and committee members: Steve Meshnick, Rick Tidwell, Marcia Hobbs, Ed Collins and Peter Gilligan. I also thank Jeff Frelinger, Carrie Barnes, Susan Jones, Sheryl Wilson, Michael Chua, David Klapper, Ivan Rusyan lab, Mike Barrett, Vicki Wingate, Stephanie Wallace, Jaina Patel, Paul Wilson and Dixie Flannery for their technical and administrative support. I especially thank: Jesse Kwiek, Jon Juliano, Charlotte Lanteri, Alisa Alker, Kirk Prutzman, Janette Stender, Paul Kurz, my parents (Donna and Tom Purfield), Toby, Holly Gentry-Bray, Sean Palmer, Heather Palmer, Tiffany Warmowski, Tracy Mazurkiewicz, Bruce Alexander, Leslie Arney and Angie Ponguta for listening.

TABLE OF CONTENTS

Page

LIST OF TABLES

LIST OF FIGURES

LIST OF ABBREVIATIONS

AFRIMS	Armed Forces Research Institute for the Medical Sciences
Asn	Asparagine
Asp	Aspartic Acid
CT	Cycle threshold
FIC	Fractional inhibitory concentration
dhfr	dihydrofolate reductase
dhps	dihydropteroate synthase
HAT	Human African trypanosomiasis
IC50	Half maximal inhibitory concentration
In vitro	In cultured parasite-infected erythrocytes
In vivo	In malaria patients
Lys	Lysine
MDR1	Multi-drug resistance One
NPP	New permeation pathway
Parasitemia	Percent red blood cells infected with parasites
PCR	polymerase chain reaction
PCP	*Pneumocystis jiroveci* pneumonia
pfcrt	Plasmodium falciparum chlroquine resistance transporter
pfmdr1	Plasmodium falciparum mult-drug resistance One
Phe	Phenylalanine
Post-culture	Parasite DNA extracted directly from cultured patient isolates
Pre-culture	Parasite DNA extracted directly from patient blood

Ser	Serine
SNP	Single nucleotide polymorphism
Thr	Threonine
Tyr	Tyrosine

CHAPTER 1
Introduction

CHAPTER 1

Introduction

Geographical distribution of malaria

Malaria is a devastating disease caused by obligate intracellular protozoa of the Plasmodium genus. Over 40% of the world's population is at risk for developing malaria, and more than 1 million deaths are attributed to the disease annually (146). There are four species of parasites that cause human malaria: *P. falciparum*, *P. vivax*, *P. malariae* and *P. ovale*. Although *P. falciparum* and *P. vivax* are the most frequent causes of malaria, *P. falciparum* is associated with most severe malaria infections and nearly all fatalities. Sub-Sarharan African children are most at risk; 18% of all deaths under the age of five years are attributed to malaria (130).

The geographical distribution of falciparum malaria is limited to that of its vector, *Anopheles* sp. mosquitoes. The best vectors are in Sub-Saharan Africa, where 70% of clinical falciparum malaria cases occur in Africa (146) (Figure 1.1).

Life cycle of *P. falciparum*

The life cycle of the malaria parasite is complex and has an integral role in the pathogenesis of malaria (Figure 1.2) (2, 37, 143). The anopheles mosquito serves as the vector with the human serving as the host (2). The parasite enters the human host as a sporozoite through the bite of a female anopheles mosquito. It undergoes asexual reproduction in hepatocytes before entering the blood stream and rapidly invading erythrocytes as merozoites. During a 48-hour period in the blood stream, the parasite matures from a merozoite to a trophozoite and finally to a multi-nucleated schizont.

During the trophozoite stage, the parasite undergoes growth, developmental gene expression, protein production, hemoglobin digestion and finally, DNA replication. The haploid DNA is replicated as the parasite advances to the multi-nucleated schizont stage. At the final stage of the 48-hour erythrocytic cycle, the multi-nucleated schizont ruptures the red blood cell, and new merozoites quickly invade uninfected erythrocytes. New merozoites develop into the sexual stage gametocytes or maintain the asexual reproductive cycle by maturing into trophozoites to perpetuate the life cycle in the host. The continuation of the asexual erythrocytic cycle causes malaria symptoms in the human host (Figure 1.2) (2, 37).

The asexual cycle is responsible for malaria morbidity and mortality, whereas the sexual stage is required for malaria transmission. Female anopholes mosquitoes ingest blood meals prior to laying eggs. When sexual-stage gametocytes are ingested, they travel to the mosquito midgut and undergo sexual fertilization to produce ookinetes. Eventually the ookinetes mature into sporozoites and travel to the salivary gland of the mosquito. Another human host is infected when the sporozoites are injected prior to the mosquito's blood meal (2, 37).

Clinical *P. falciparum* malaria presentation and diagnosis

Clinical malaria results from the continuation of the asexual erythrocytic cycle of the parasite in the human host (6). Typical malaria disease includes a latent (asymptomatic) period followed by symptomatic disease. The latent period can be as short as six days from the initial bite of an infected mosquito to clinical symptoms (17). During the asymptomatic period, parasites replicate in hepatocytes after which they infect erythrocytes. By the first asexual replication cycle in erythrocytes, infected individuals experience typical malaria paroxysms: shaking chills followed by spiking fevers up to 106^{o}F and finally, extreme sweating (6).

The disease progresses differently among partially immune individuals and naïve individuals lacking protective immunity from repeated exposure. Naïve individuals are more sensitive to parasitemia levels and experience febrile illness with as few as 10 parasites/μL of blood (148). In contrast, individuals with partial immunity typically have a higher parasite threshold, accommodating up to 1000 parasites/μL of blood before onset of fever. Subsequently, patients with partial immunity experience a delay in the onset of typical symptoms associated with the high parasitemia in uncomplicated malaria such as: headache, fatigue, abdominal pain, myalgia, nausea, diarrhea and irregular, but persistent fever (61).

Malaria paroxysms may occur at regular intervals as the parasite population becomes synchronized. High fever is thought to aid in synchronizing the parasites to a 48-hour cycle with coordinated schizont rupture and subsequent merozoite release (80, 81). Since mature erythrocytic-stage schizonts release between 10 and 32 new merozoites, parasitemia increases about 10-fold every 2 days if left untreated (61). Thus, parasitemia increases in a short period of time, and subsequent clinical complications associated with severe malaria appear 4-6 days after the onset of initial malaria symptoms (61). Treatment within 6 days of the onset of the uncomplicated malaria symptoms can prevent severe malaria, and a full recovery may be expected within a few days (61).

Severe malaria may progress undetected from uncomplicated malaria, and the symptoms vary among adults and children. Naïve individuals, such as African children, are most susceptible to severe malaria complications. Children most often experience severe anemia with rare episodes of renal failure and pulmonary edema. However, adults are more likely to experience renal failure and pulmonary edema (61, 136). Typical symptoms of severe malaria, regardless of patient age, include thrombocytopenia (116, 145), respiratory distress

(94), acidosis (51, 116), or cerebral malaria which often leads to coma, convulsions and death (6, 38, 94, 102, 149).

The gold standard for malaria diagnosis is the identification of parasites in a Giemsa-stained blood smear. Thick and thin peripheral blood smears are used to assess the parasite density, species and disease severity (6, 142). Other diagnostic methods include rapid antigen tests and polymerase chain reaction (PCR), but these have limitations due to cost, time and specificity (6).

Mechanisms of action and resistance for antimalarial drugs

In the middle of the 20th century, health experts believed malaria could be successfully eradicated. At the time, malaria had characteristics that made eradication seem possible, including the absence of an animal reservoir to harbor parasites and drugs that effectively cured infections to interrupt transmission (152). Since that optimistic prediction, the characteristics of the parasite have changed. Today, *P. falciparum* has developed resistance to nearly all antimalarial drugs in use (reviewed in (152, 172)). Resistance to affordable drugs, such as chloroquine, is present in practically all areas endemic with falciparum malaria (reviewed in (152, 167, 172)) (Figures 1.1 and 1.3). The rapid emergence and spread of antimalarial drug resistance has forced researchers to evaluate the antimalarial mechanisms of action and resistance in an effort to effectively treat patients to prevent escalation of the current situation with drug resistance (110).

The most widely used anti-malarial drugs are classified by their mode of action and structure. The class of antimalarial compounds known as the antimetabolites include pyrimethamine, proguanil and sulfonamides. The modes of action for these drugs are well established. Antimetabolites inhibit the folate synthesis pathway enzymes dihydropteroate

synthase (DHPS) and dihydrofolate reductase (DHFR). The folate pathway is necessary for pyrimidine synthesis by the parasite. Mutations in the genes encoding the drug target, DHPS or DHFR, alter the binding affinity and reduce parasite sensitivity to the drug (37). The mutations are used as molecular markers for decreased parasite susceptibility to antimetabolites (166).

For many antimalarials, the modes of action as well as the mechanisms of resistance remain unknown in spite of effective chemotherapeutic properties. This is the case for artemisinin derivatives and quinoline-containing drugs, which include chloroquine, mefloquine, halofantrine and amodiaquine (reviewed in (88, 91, 110).

The peroxide, artemisinin, is a relatively new antimalarial derived from *Artemisia annua*, in the Asteraceae plant family (173). Artemisinin is the parent compound of derivatives synthesized to improve administration by oral, rectal and parenteral routes (reviewed in (173)). Multiple mechanisms of action have been proposed for artemisinin compounds, including drug interaction with heme to form toxic free radicals and inhibition of the parasite sarcoplasmic endoplasmic reticulum ATPase (49, 101, 156). The latter theory is supported by evidence that mutations in the putative ATPase target can alter artemisinin susceptibility of parasites in culture (156). However, there is currently no evidence for in vivo resistance (173).

Chloroquine is a synthetic 4-aminoquinoline compound with an unknown mechanism of action. Chloroquine was the first antimalarial synthesized and is still used today because of its cost-effectiveness (110). Despite its widespread use and 70+ year history, the mechanism of chloroquine action is not fully understood (71, 110). Although the killing mechanism is debated, there is some agreement that the drug targets the parasite food vacuole.

Chloroquine, a weak base, accumulates in the parasite food vacuole and alters the pH of the acidic organelle (176). In the parasite food vacuole, enzymes digest hemoglobin into heme (ferriprotoporphyrin IX), which is toxic to the parasite. Heme is detoxified via biocrystallization into hemozoin, and disruption of the process that converts hemoglobin to heme to hemozoin has detrimental effects on the parasite (27). Chloroquine binds heme and interrupts the heme polymerization process, and the resulting heme-chloroquine complex is toxic (55, 150).

Further evidence that the food vacuole is an important chloroquine target was provided by the recognition that mutations in the *pfcrt* gene, which encodes the *Plasmodium falciparum* chloroquine resistance transporter, confer decreased susceptibility to chloroquine (54). Pfcrt is a transmembrane protein on the surface of the food vacuole (54). Single nucleotide point (SNP) mutations in *pfcrt* results in amino acid substitutions in Pfcrt, and allow leakage of chloroquine out of the food vacuole, mitigating its effect on vacuolar pH and its ability to prevent hemozoin synthesis (71, 131, 132, 141, 161). Although the specific role of Pfcrt in drug susceptibility remains unresolved, twenty mutations in the *pfcrt* gene have been associated with decreased in vitro chloroquine sensitivity (31). Only one mutation, resulting in a change from lysine to threonine at amino acid 76 ($Lys^{76} \rightarrow Thr^{76}$), has been linked to clinical treatment failure with chloroquine (Table 1.1). The Thr^{76} substitution is used as a molecular marker for chloroquine resistance. Removal of the Thr^{76} mutation by allelic exchange restores in vitro sensitivity in parasites and confirms the importance of this mutation in chloroquine sensitivity (83).

Another gene thought to be associated with drug resistance is *pfmdr1*. *pfmdr1* encodes the parasite food vacuole transport protein, P-glycoprotein homologue 1 (Pgh1), which is a

homologue of the human P-glycoprotein, encoded by human *multi-drug resistance-1* (*MDR1*). Human P-glycoproteins modulate susceptibility to multiple drugs in mammalian cells (73, 128).

Mutations in *pfmdr1* are associated with altered parasite susceptibility to multiple drugs, including chloroquine and mefloquine (35). A *pfmdr1* SNP resulting in an amino acid substitution ($Asn^{86} \rightarrow Tyr^{86}$) in Pgh-1 was found to be associated with chloroquine treatment failure in patients (Table 1.1) (42). However, other studies show that while the $Asn^{86} \rightarrow Tyr^{86}$ substitution in *pfmdr1* is correlated with increased susceptibility to chloroquine in vitro, it is associated with decreased susceptibility to mefloquine (114).

Mefloquine, an aryl amino alcohol compound, has been very effective as an antimalarial. The drug has a long terminal half-life, which makes it an ideal candidate for prophylaxis, because one dose can protect for a week. However, the long half life has also led to the rapid development of resistance when used in endemic areas for falciparum malaria treatment (37, 163).

Although the mefloquine mechanism of action has not been elucidated, multiple mechanisms of resistance have been described. Multiple SNPs in *pfmdr1* are associated with decreased parasite susceptibility to mefloquine (Table 1.1) (33, 118). Also, increased copies of *pfmdr1* in the falciparum genome are correlated with decreased mefloquine susceptibility (118, 120). Taken together, these observations suggest a role for *pfmdr1* in drug susceptibility.

***pfmdr1* is a modifier of drug susceptibility**

Since its discovery, *pfmdr1* has been used as a marker of parasite susceptibility to structurally diverse antimalarials, including chloroquine, a 4-aminoquinolone and aryl amino

alcohols, such as mefloquine, quinine and halofantrine, quinine, and lumafantrine (124). The Pgh1 product of *pfmdr1* is thought to regulate intracellular drug or substrate concentrations (33). Therefore, *pfmdr1* gene amplification or structural modifications to Pgh1 via mutations are likely to affect intracellular drug concentrations and parasite susceptibility.

To link *pfmdr1* gene amplification with a physiological mechanism of drug resistance, *pfmdr1* copy number was assessed with transcript levels (170, 171). A mefloquine resistant *P. falciparum* strain contained more copies of the *pfmdr1* gene as well as *pfmdr1* mRNA transcripts (170, 171). Further, Rohrbach, et al., correlated increased *pfmdr1* copy number with Pgh1 protein expression and function in vitro (126). Using a fluorescent substrate, Rhorbach, et al., found that Pgh1 acts as a transporter for substrates into the food vacuole (126). This supports the theory that Pgh1 regulates substrate concentrations in the food vacuole, suggesting that modifications of the gene copy number or protein structure may directly affect intracellular drug distribution (126). The correlation between gene copy number, transcript levels and protein levels has been difficult to show in clinical samples because large quantities of freshly harvested parasites are required to obtain adequate mRNA and protein for analysis.

In epidemiological studies, *pfmdr1* amplification correlates with resistance to multiple antimalarials. Therefore, increased *pfmdr1* gene copy number is considered a molecular marker for resistance to antimalarials, including mefloquine, quinine, halofantrine and lumafantrine (4, 170). In laboratory strains and clinical isolates, there is a correlation between in vitro mefloquine resistance and resistance to halofantrine, lumafantrine and quinine, suggesting the drugs may have a similar mechanism of resistance, such as increased *pfmdr1* copy number (34, 58, 108, 111, 164, 171).

SNPs in *pfmdr1* are additional molecular markers for mefloquine resistance in parasites, providing further evidence that *pfmdr1* is important for resistance. Extensive sequencing of *P. falciparum* isolates revealed nonsynonymous point mutations resulting in codon changes at 5 positions (Figure 1.4) (56). The five key amino acid substitutions are: $Asn^{86} \rightarrow Tyr^{86}$, $Tyr^{184} \rightarrow Phe^{184}$, $Ser^{1034} \rightarrow Cys^{1034}$ and $Asn^{1042} \rightarrow Asp^{1042}$, $Asp^{1246} \rightarrow Tyr^{1246}$ (Figure 1.4 and Table 1.1). These mutations were first noted in studies of the role of *pfmdr1* in chloroquine resistance in vitro (56). Further in vitro studies showed a correlation between one or more of these SNPs and resistance to additional antimalarials with laboratory strains (56, 111, 124, 157, 160).

Assessments of malaria patient samples for an association between decreased drug susceptibility and mutations revealed discordant findings (47, 48, 75, 99, 114, 120). For example, Wilson et al., found no association between these previously described 5 alleles (Table 1.1) and decreased susceptibility to mefloquine and halofantrine in clinical samples (171). In contrast, Duraisingh, et al. showed a correlation between increased susceptibility to mefloquine and chloroquine and the presence of the *pfmdr1* Tyr^{86} mutation (47). Finally, the amino acid substitution at Phe^{184} was associated with decreased mefloquine susceptibility in work by this author (114). These conflicting reports suggest additional factors may contribute to drug sensitivity in vitro.

When *pfmdr1* allelic variants were assessed with respect to patient outcome, results were often inconsistent and varied geographically (Table 1.2). This may be due, in part, to the distribution of the mutations in parasite populations. For instance, Tyr^{86} and Phe^{184} mutations have been found in Asia, Africa and South America. In contrast, mutations at amino acid positions 1034, 1042 and 1246 are most prevalent in South America (reviewed in (174)).

Factors such as variable rates of transmission and drug pressure may influence the geographical distribution of parasite genotypes (174).

Taken together, studies to date have failed to conclusively identify SNPs in *pfmdr1* as a mechanism of antimalarial resistance and treatment failure; however the high prevalence of these mutations and the associations with drug resistance and treatment failure cannot be dismissed entirely. Additional studies with larger numbers of samples from geographically diverse settings are needed. In Chapter 2 of this thesis a new real time PCR method for assessing *pfmdr1* genotype directly from patient blood is presented. This method is amenable for high-throughput analysis of large numbers of samples, which would better define an association between SNPs and drug susceptibility.

Molecular surveillance of antimalarial drug resistance

As antimalarial resistance emerges de novo and spreads rapidly with disease transmission, it is increasingly important to use surveillance tools to monitor drug susceptibility in parasite populations. The gold standard for monitoring drug efficacy is assessing clinical treatment outcome. A more timely method for surveying resistance is to examine parasite susceptibility to antimalarials in vitro (29, 140). The data collected in vitro may predict impending drug resistance in patients (23, 127).

Molecular markers for drug resistance are an additional tool for surveillance of drug susceptibility. The prevalence of molecular markers associated with drug resistance will yield insight into the evolution of parasite genotypes and the spread of resistance between geographical regions (72, 106).

Assessment of drug susceptibility and molecular markers provide insight about the temporal evolution and geographical spread of parasite populations exhibiting drug resistance

(140). Healthcare officials evaluate all available surveillance data to adjust policy regarding antimalarial treatment. Proper action in a timely manner will thwart the spread of antimalarial drug resistance, prolong the use of treatments and ultimately, reduce mortality.

Artemisinin combination therapy to prevent resistance

Because drug resistance develops quickly, the World Health Organization (WHO) recommends the use of drug combination therapy (1, 50). The basis for combination therapy incorporates multiple antimalarial drugs with indifferent or synergistic effects when used in combination for parasite inhibition (168). Ideal candidates for combination therapy exhibit independent modes of action and unique biological targets (1, 168). Further, drugs with similar pharmacokinetic profiles or plasma half-life will be eliminated at the same rate. Simultaneous elimination of multiple drugs ensures the parasite is not exposed to sub-therapeutic levels of a single drug as with monotherapy. With monotherapy, sub-therapeutic levels of a the partner drug alone promotes selection for resistant parasites because the drug concentration is too low to eliminate the parasite population (64).

Currently, one candidate for use in combination therapy is artemisinin and its derivatives: artesunate, dihydroartemisinin and artemether. When used as monotherapy in a 3-day treatment regimen, artemisinin has an incomplete cure rate (~50%) with no clinical evidence of resistant parasites (reviewed in (100)). However, artemisinin compounds used in combination therapy with partner drugs for 3-day dosing regimens are highly effective and are the current preferred basis for combination therapy (1, 23, 119). Artemisinins have short plasma half-lives; combining artemisinin with a partner drug that has a longer plasma half life will ensure long suppressive treatment after the initial rapid decrease in parasitemia from

artemisinin, however this is a conundrum, since it potentially promotes emergence of resistant parasites to the longer-acting partner drug (reviewed in (173), (1, 64)).

The pharmacokinetics of artemisinin combination therapy could allow for resistance to the longer acting partner drug to develop. Once artemisinin is rapidly eliminated, the partner drug will be present in sub-therapeutic levels in the patient plasma The low levels of parasites that may exist in the patient may develop resistance to the longer acting partner drug that is, essentially, monotherapy at this point (68). However, the effect of artemisinin combination therapies with mismatched pharmacokinetic profiles on the selection of resistant parasites to the partner drug has yet to be determined in patients, and artemisinin in combination remains the preferred therapy (1, 79). Additional clinical trials and in vitro susceptibility testing are needed to monitor the effects on developing resistance to artemisinin and partner drugs with longer plasma half lifes.

A need for new antimalarial drugs

There is an increasing need for new antimalarial drugs to use for combination therapy against malaria. With the exception of artemisinin compounds, all currently available antimalarials have been used as monotherapy, and resistant parasites have been detected in patient isolates (9).

Another factor driving the need for new antimalarials is cost per treatment. Drugs developed through public-private partnerships will be more affordable than those developed by pharmaceutical companies that focus development of antimalarials for the population needing prophylaxis, such as travelers visiting or working in endemic regions (9). In addition to reduced cost, new drug entities used for combination therapy may offer another

advantage. Chemical entities that have not been previously used for monotherapy to treat malaria may last langer in the absence of pre-existing resistance (1).

Aromatic diamidines have antimalarial activity

Pentamidine, [1,5-di(4-amidinophenoxy)pentane] (Figure 1.5a), a dicationic diamidine, has been used for clinical treatment of protozoan infections such as leishmaniasis and Human African trypanosomiasis (HAT) (165). Pentamidine also has activity against *Plasmodium falciparum*, however the drug is not orally bioavailable and has considerable side effects, including renal toxicity and cardiotoxicity (5, 21, 52). Therefore, pentamidine has been passed over as a potential malaria therapeutic in favor of drugs with oral bioavailability and fewer side effects (21). In spite of the side effects and need for parenteral administration, it is still a first line treatment for early-stage HAT and a second line drug for antimony-resistant visceral leishmaniasis and *Pneumocystis jiroveci* pneumonia (PCP) (21, 165). The synthesis of new pentamidine structural analogues for alternative treatments of HAT has introduced a class of broad-spectrum antimicrobials with orally active prodrugs lacking the side effects associated with pentamidine (13, 122). This class of aromatic diamidines inspired by pentamidine is being investigated for therapeutic use for malaria, PCP and leishmaniasis, in addition to HAT (13, 165).

Diamidine mechanisms of action for antimicrobial activity

The mechanism of action of pentamidine and diamidine compounds in general remains unknown (21). Studies have provided multiple theories for the selective inhibitory action of diamidines in a variety of protozoan, including *Giardia lamblia*, trypanosomes and *P. falciparum*. These include DNA-binding and inhibition of replication enzymes (7, 11, 13, 98), collapse of mitochondrial membrane potential and subsequent cellular respiration

inhibition (86, 158), heme binding (147), inhibition of peptidase activity (103) and disruption of calcium homeostasis through acidocalcisome localization (14). These investigations suggest pentamidine may have multiple biological targets across a broad range of protozoan (133).

Pentamidine is the diamidine most studied, however mechanistic studies of pentamidine in Plasmodium are limited. Pentamidine has clear antimalarial activity with a half-maximal inhibitory concentration (IC50) value comparable to those of standard antimalarial agents (13, 147). One debated mechanism of action for pentamidine in Plasmodium is the inhibition hemozoin formation in the parasite food vacuole. When added to parasite lysate in vitro, pentamidine binds the toxic heme (ferriprotoporphyrin IX) molecule that is produced during hemoglobin metabolism. By binding heme, pentamidine inhibits the parasite's ability to crystallize the molecule into a nontoxic form, hemozoin (147). Pentamidine and chloroquine exhibit similar binding affinities for heme (K_d=2.9μM and 2.5μM, respectively) (147, 150). Structurally similar diamidines with antimalarial activity, including propamidine and stilbamidine, were also found to bind heme in the presence of parasite lysate at concentrations in the micromolar range, suggesting additional diamidines may bind heme as well (147).

The uptake and transport of pentamidine has also been studied to determine the mechanism of action. Pentamidine is taken up by parasite-infected red blood cells, but not by uninfected red blood cells. Investigations using tritiated pentamidine show drug concentrations in parasite-infected cells are 500-fold greater than in the extracellular media within three hours of drug exposure (147).

It has been suggested that pentamidine is transported across the erythrocyte membrane by the new permeation pathway (NPP), also known as the plasmodial surface anion channel (147). Parasite-infected erythrocytes transport a broad range of solutes across the host cell membrane through pores, collectively referred to as the NPP (78). It is unknown whether the channel is composed of parasite-produced proteins exported to the erythrocyte membrane or erythrocyte proteins that are remodeled to form the pores of the NPP (76). The NPP is believed to primarily function as an anion channel, however permeability to cations and nonelectroytes has been noted (76-78, 147). The destination of solutes transported by the NPP is unknown. The NPP may deposit solutes into the erythrocyte cytoplasm or into the tubovesicular membrane, which is a network of tubular membranes connecting the erythrocyte membrane directly to the parasitophorous vacuole membrane (40, 87). Inhibitors of the NPP block pentamadine uptake by the parasite-infected red blood cell, suggesting a role for the NPP in drug transport (147).

In addition to heme binding, pentamidine and other diamidine compounds bind nucleic acids. Dicationic diamidine compounds, including pentamidine, bind to the minor groove of DNA with an affinity for AT-rich sequences (11, 179). This attraction is facilitated by the electrostatic interaction between the positively-charged diamidine molecule and the negatively charged nucleic acids (98). Plasmodium, as well as leishmania and trypanosomes, contain abundant AT rich nucleic acid sequences, suggesting diamidine compounds may be particularly effective against these organisms if nucleic acid-binding is a mechanism of action (8, 57, 93).

DNA binding affinity is associated with biological activity of diamidines in protozoa and tumor cells (11, 32, 85). DNA binding affinity is directly correlated to DNA topoisomerase

II inhibition in *Giardia lamblia* in vitro (12, 19). Inhibition of DNA topoisomerase II is believed to inhibit nuclear DNA synthesis and may serve as the mechanism of killing for dicationic diamidines in *G. lamblia* (12).

Subcellular localization studies show diamidine compounds localize to the nucleus of trypanosomes and tumor cells, further suggesting nucleic acids may be a target in the cell (85, 97). Nuclear localization is dependent on the structure of diamidine compounds and compounds with higher affinity for binding DNA are more likely to localize to the nucleus (85, 105).

DB289 is the orally active prodrug of the novel antimicrobial agent, DB75

New dicationic diamidines were synthesized in an effort to improve oral bioavailability and reduce toxicity associated with pentamidine. DB75, [2,5-bis(4-amidinophenyl)furan] (Figure 1.5b), also known as furamidine, has impressive activity against a broad range of microbes, including *P. falciparum*. In some models, DB75 shows improved antimicrobial activity with reduced toxicity over pentamidine (19, 122, 129). However, DB75 has poor oral activity when administered alone (180). The positively charged cationic moieties of DB75 may prevent drug transport across the intestinal epithelium (182). To use DB75 as a clinical therapeutic, an orally active pro-drug was synthesized. The pro-drug, DB289, [2,5-bis-(4-amidinophenyl)furan bis-*O*-methylamidoxime], may be administered orally and is metabolized to the active form, DB75 (Figure 1.5c) (180, 181). The biotransformation process of DB289 to DB75 in the human liver consists of three *O*-demethylation reactions catalyzed by the Cyp4F enzyme subfamily and three *N*-dehydroxylation reactions catalyzed by cytrochrome b_5 and NADH-cytochrome b_5 reductase (135, 162).

DB289 is currently the lead diamidine compound for therapeutic treatment against HAT, PCP and malaria (personal communication, Richard R. Tidwell). The pro-drug is in Phase III clinical trials for treatment of acute HAT and PCP. DB289 is in Phase II clinical trials for both prophylaxis and treatment of acute, uncomplicated *P. vivax* and *P. falciparum* malaria (personal communication, Richard R. Tidwell). No serious adverse side effects were observed in human clinical trials for either HAT or PCP (177). For the treatment of HAT, DB289 has achieved a 95% cure rate (personal communication, Richard R. Tidwell).

The pro-drug has an impressive 96% (22 of 23 patients) cure rate for acute uncomplicated falciparum malaria when used as monotherapy (100mg, twice daily for 5 days) to treat patients in a Bangkok, Thailand (178). No serious adverse side effects were noted, and DB289 has proceeded to Phase IIb clinical trials to determine the ideal treatment regimen in malaria. The efficacy of DB75 is also being studied in combination therapy with artesunate, an artemisinin derivative (personal communication, Richard R. Tidwell).

Despite the high efficacy of DB289 in patients, the mechanism of action of DB75 is unknown. Chapter 3 of this dissertation will address the mechanism of action for DB75 in *P. falciparum*.

Dissertation objectives and significance

This dissertation work examines mechanisms of resistance in *P. falciparum* and the mode of action for the novel diamidine, DB75. The major objectives of this dissertation were 1) to develop real time PCR methods to evaluate genotypic differences in drug resistant parasites from clinical samples; 2) to investigate the mechanism of action for DB75 in *P. falciparum* in vitro; and 3) to identify potential therapeutic partners for DB289 through drug combination studies in vitro.

First, a new method for high throughput analysis of parasite mutations associated with drug resistance will advance the field of malaria drug surveillance. Identification of drug resistant parasite populations in advance of clinical trials will expedite policy changes regarding treatment regimens.

Second, identification of the DB75 mechanism of action will have important implications for the clinical use of DB289 as well as other dicationic diamidines in development for a similar use. The mechanism will determine how DB289 may be best used in combination therapy to avoid development of resistance. Further, the mode of action will be used to determine how parasite resistance will develop against DB289.

Finally, the evaluation of DB75 in combination with other antimalarial agents in vitro will yield a greater understanding of the drug's mechanism of action against *P. falciparum*. In addition, these combination studies will determine how parasite inhibition is affected by DB75 in the presence of a second drug. Potential partner drugs for combination therapy may be identified through these interactions

Figure 1.1: Geographic distribution of *P. falciparum* malaria risk. Global risk of transmission is shown with intensity of green color. The darkest green indicates hyperendemic or holoendemic regions. Global distribution of drug resistance from sentinel sites to 2004 (146).

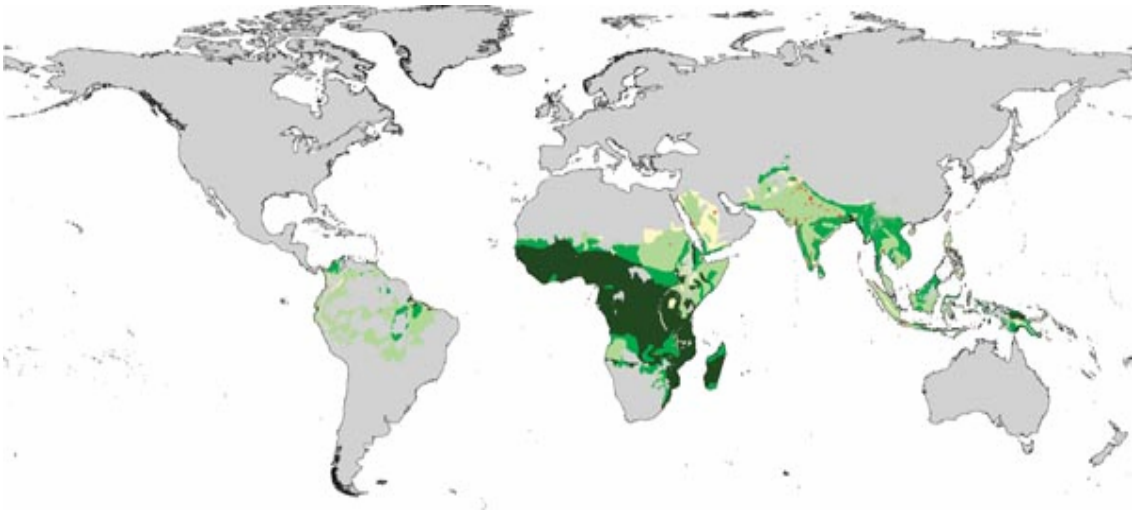

Figure 1.2: Life cycle of the *P. falciparum* parasite. The plasmodium parasite has a complex life cycle between the human host and the mosquito vector. This includes the sporogenic cycle in the mosquito and both the liver and erythrocytic cycles in the human host.

Source: Centers for Disease Control and Prevention: (http://www.dpd.cdc.gov).

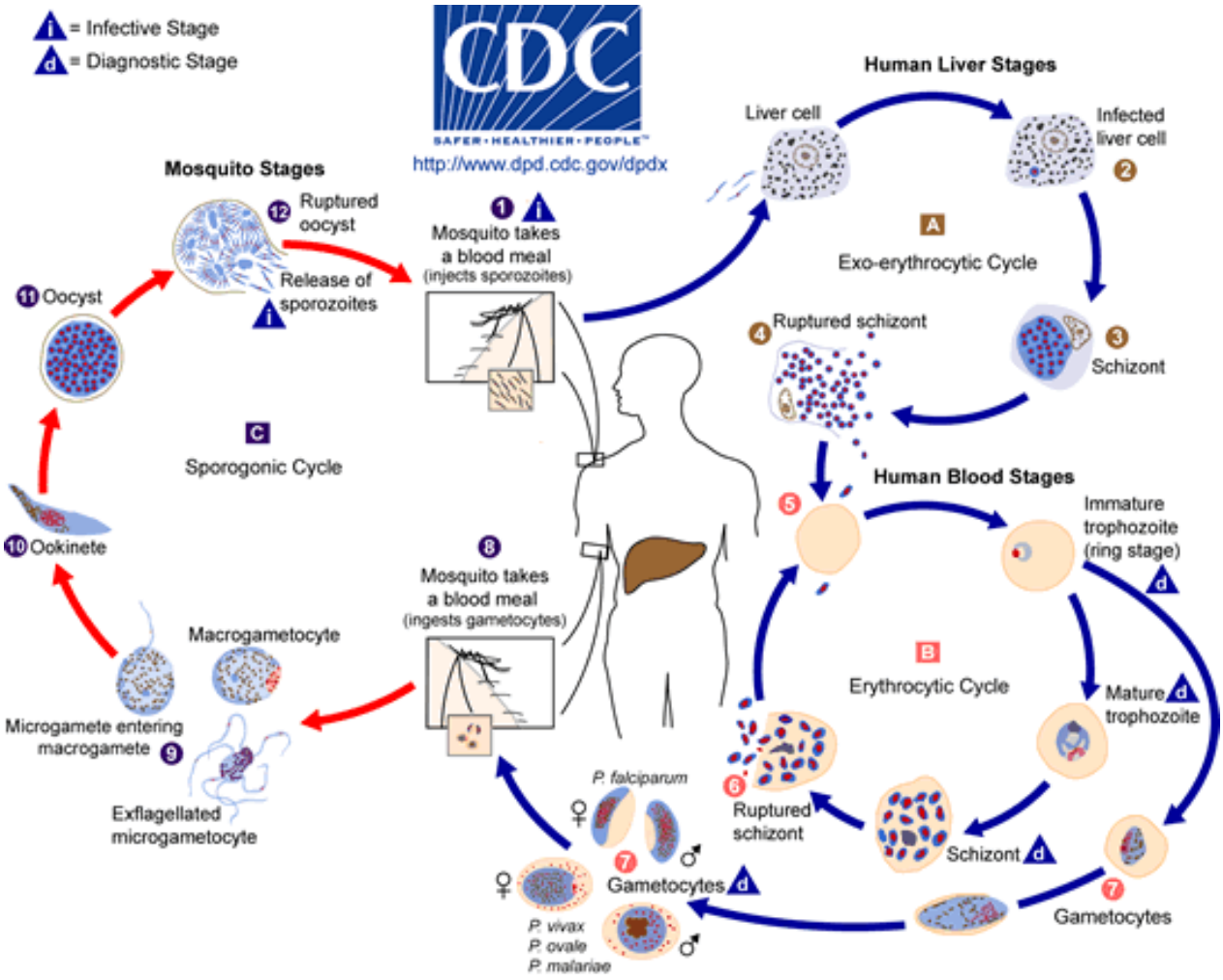

Figure 1.3: Worldwide distribution of *P. falciparum* drug resistance. Decreased susceptibility to chloroquine (pink triangle), sulfadoxine-pyramethamine (green circle), and mefloquine (yellow star) is widely reported in areas of high malaria transmission (shaded) (50).

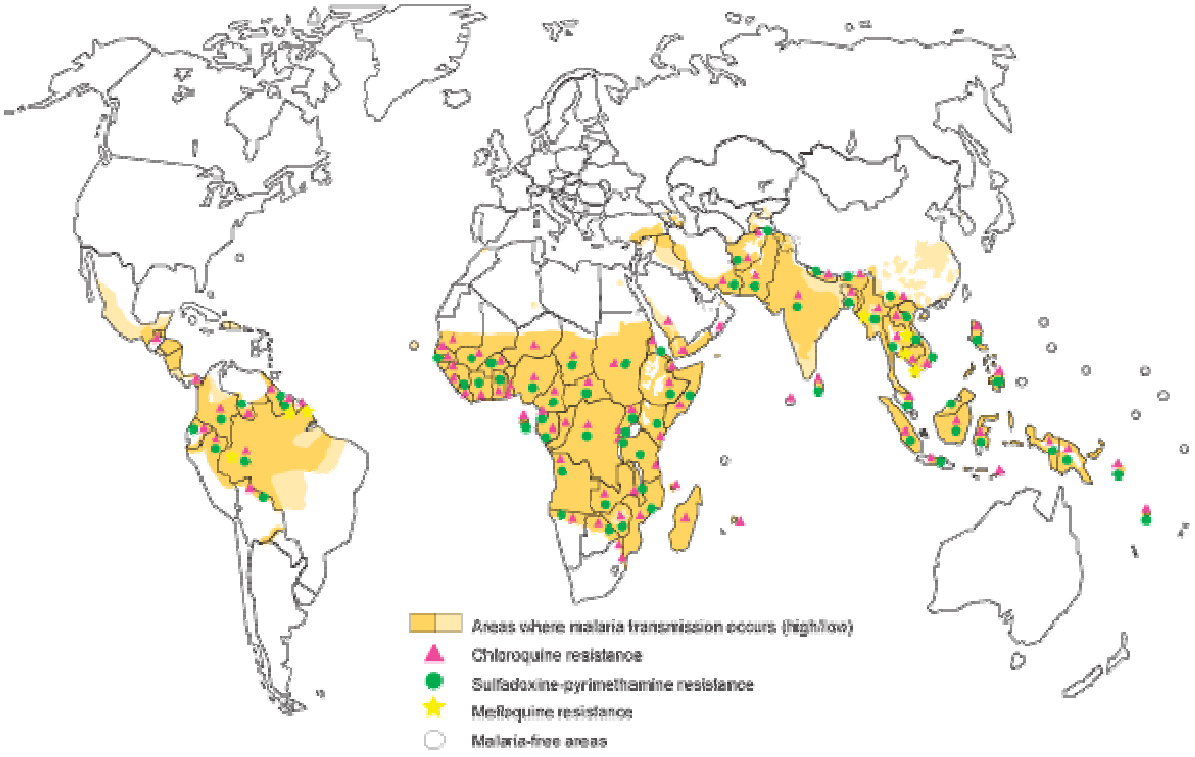

Figure 1.4: Model of P-glycoprotein homologue-1 protein encoded by *pfmdr1*. The model shows 12 predicted transmembrane domains for this transport protein with locations of single nucleotide polymorphisms and resulting amino acid changes (45).

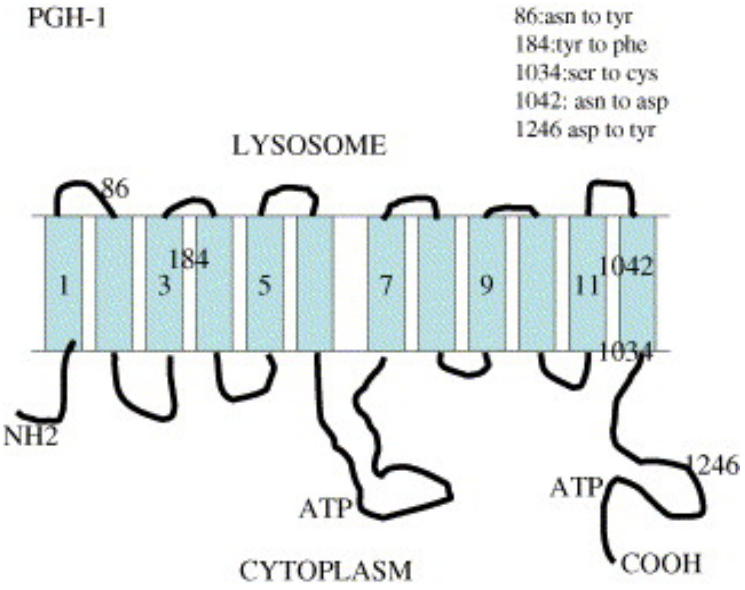

Table 1.1: Important mutations associated with decreased antimalarial susceptibility

Gene	Gene Product	Important amino acid substitutions	Associated Decreased Drug Susceptibility[a]
pfcrt	*Plasmodium falciparum* chloroquine resistance transporter	Lys^{76} to Thr^{76}	Chloroquine
pfmdr1	P-glycoprotein homologue 1	Asn^{86} to Tyr^{86}	Mefloquine, Halofantrine, Lumafantrine, Quinine, Chloroquine
		Tyr^{184} toPhe^{184}	Mefloquine, Halofantrine, Lumafantrine, Quinine
		Ser^{1034} to Cys^{1034}	Mefloquine, Halofantrine, Lumafantrine, Quinine
		Asn^{1042} to Asp^{1042}	Mefloquine, Halofantrine, Lumafantrine, Quinine
		Asp^{1246} to Tyr^{1246}	Mefloquine, Halofantrine, Lumafantrine, Quinine

[a] Determine by in vitro susceptibility testing

Table 1.2: *Pfmdr1* single nucleotide polymorphisms resulting in amino acid substitutions in Pgh-1 are geographically linked to antimalarial treatment failure in clinical studies

Drug	Southeast Asia[a]	Sub-Saharan Africa[b]
Mefloquine	No correlation (115) Tyr^{86} (114) Phe^{184} with Cys^{1034} or Asp^{1042} (114) Phe^{184} (75)	
Chloroquine	Tyr^{86} with *pfcrt* Lys^{76} (16) Tyr^{86} (42)	Tyr^{86} (44, 46, 47, 109) No Correlation (63) Tyr^{86} with *pfcrt* Lys^{76} (109, 154)
Amodiaquine		Tyr^{86} (43, 46, 62, 66) Tyr^{1246} (43, 66) Tyr^{86}/ Tyr^{184}/ Tyr^{1246} (66, 67)
Artemether-Lumafantrine (Coartem)		Phe^{184} (144)
Amodiaquine-Artemisinin		Tyr^{86}(107) Tyr^{1246} (66, 107)

[a] Single nucleotide polymorphisms correlated with antimalarial drug resistance in Southeast Asia

[b] Single nucleotide polymorphisms correlated with antimalarial drug resistance in Africa

Figure: 1.5: Chemical structures of dicationic diamidines with antimalarial activity. a) Pentamidine [1,5-di(4-amidinophenoxy)pentane]; b) DB75 [2,5-bis(4-amidinophenyl)furan]; c) DB289 [2,5-bis(4-amidinophenyl)furan bis-*O*-methylamidoxime]

a.

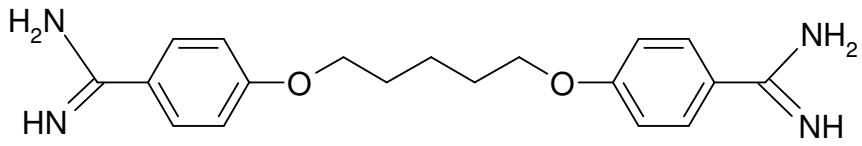

b.

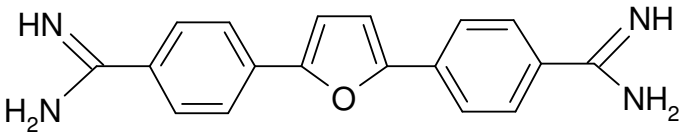

c.

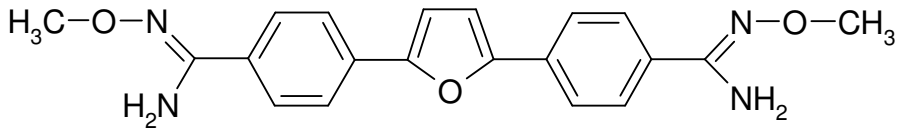

CHAPTER 2

A New Method for Detection of *pfmdr1* Mutations in *Plasmodium falciparum* DNA Using Real Time PCR

PREFACE

This chapter was published in Malaria Journal in 2004 under the same title: A New Method for Detection of *pfmdr1* Mutations in *Plasmodium falciparum* DNA Using Real Time PCR (121). Additional contributing authors include: Amy Nelson, Anita Laoboonchai, Kanungnij Congpuong, Phillip McDaniel, R. Scott Miller, Kathy Welch, Chansuda Wongsrichanalai and Steven R. Meshnick.

I contributed to this work through the design of the real time PCR assay and analysis of parasite DNA samples with real time PCR and standard PCR. The primary author is also responsible for data analysis, including statistics and the preparation of the manuscript for publication.

For publication in this dissertation minor changes were made to this article. These changes do not alter the conclusions drawn by the authors at the time of the original publication. Changes include:

- Discussion Section was enhanced
- Table 2.3: Two samples are described as 184^{Phe} (mutant) in post-culture DNA but 184^{Phe} and 184^{Tyr} (mixed infection) in DNA extracted directly from patient blood.
- Table 2.4: The specificity of real time PCR for detecting Asp^{1042} is 95% (60/63)

The results from epidemiology studies related to these samples evaluated by real time PCR are included in Nelson, et al., 2005, and Pickard et al., 2003, (104, 114).

CHAPTER 2

A New Method for Detection of *pfmdr1* Mutations in *Plasmodium falciparum* DNA Using Real Time PCR

Introduction

The increasing prevalence of multi-drug resistant parasites threatens to impede efforts to control malaria world-wide (172). Current in vitro and in vivo methods to monitor the emergence of drug resistance are difficult, costly and labor-intensive. Molecular methods could prove to be useful alternatives (117).

For *Plasmodium falciparum*, the *pfmdr1* gene product, Pgh1, is thought to play an integral role in the mechanism behind parasite resistance to multiple malarial drugs (124). Both increased gene copy number and SNPs have been associated in epidemiological studies with changes in sensitivity to chloroquine and mefloquine (reviewed in (152, 166, 172)). In two studies from South-east Asia, both increased *pfmdr1* gene copy number and SNPs have been associated with in vitro resistance to mefloquine (114, 118). The allelic variation of *pfmdr1* and its association with drug resistance is geographically varied. For instance, Tyr^{86} and Phe^{184} mutations have been found in Asia, Africa and South America. Contrary, mutations at amino acid positions 1034, 1042 and 1246 are most prevalent in South America (reviewed in (174)). The molecular physiology of these point mutations has not been elucidated, however epidemiological evidence suggests a strong association between their existence and drug sensitivity (174). The extent of the significance of *pfmdr1* allelic variations as molecular

markers of drug resistance may be better discerned using temporal and geographical data collected from surveillance of parasite populations (140). With adequate surveillance data, healthcare officials may evaluate and adjust antimalarial treatment policy as necessary. On an individual basis, a rapid detection method could be used to predict treatment outcome and the appropriate antimalarial regimen may be administered.

A real-time PCR assay has been developed for the rapid detection of *pfmdr1* SNPs. This assay was developed to be used in conjunction with a previously developed assay for *pfmdr1* gene copy number (114) to assess molecular markers as predictors of mefloquine failure in a clinical study that took place in Sangkhlaburi, Thailand, in 2001–2.

Numerous studies have shown discrepancies between in vitro and in vivo tests for antimalarial drug resistance (125, 138, 151). In order to understand why, *pfmdr1* genotypes were determined directly from patient blood and from cultures derived from those patients and compared.

Materials and Methods

Patient samples

This study received ethical approval from the University of North Carolina IRB and the Thai Ministry of Public Health. Patients presenting with slide-confirmed falciparum malaria to the free Ministry of Public Health malaria clinic or the Kwai River Christian Hospital clinic in Sangklaburi, Thailand from during July 2001 – August 2002 were enrolled. Patients with vivax infections, history of anti-malarial drug use within the past two weeks, bleeding tendency (by self-reported history or based on medical records), or severe/complicated malaria requiring prompt medical management for life support were excluded. In total, 74 patients consented. Blood samples were taken, aliquoted, stored in liquid nitrogen, and

transported to the Armed Forces Research Institute for the Medical Sciences (AFRIMS) in Bangkok. At AFRIMS, aliquots were thawed for in vitro culture. 59 of the 74 patient blood samples were successfully cultured as previously described (Figure 2.1) (114, 155). Parasites were cultured for between 2 and 188 days (mean = 38.5; median = 23). DNA was extracted from patient blood ("pre-culture") and cultured parasites ("post-culture") using the QiaAmp DNA Blood Minikit Blood and Body Fluid Spin Protocol (Qiagen, Valencia, CA) and then shipped on dry ice to the University of North Carolina.

Standard PCR

DNA was PCR-amplified using a MJ Thermocycler (MJ Research, Waltham, MA) as previously described (114). DNA sequencing was performed at the University of North Carolina Sequencing Core facility using a 3100 Genetic Analyser (Applied Biosystems, Foster City, CA). The sequencing reaction was done using the ABI PRISM™ BigDye™ Terminator Cycle Sequencing Ready Reaction Kit with AmpliTaq® DNA Polymerase, FS (Applied Biosystems).

Real-time PCR

For real-time PCR, pre-culture DNA and post-culture DNA were genotyped using an Applied Biosystems Prism 7000 Sequence Detection System (Applied Biosystems). This assay uses sequence-specific fluorescently-labeled minor groove binder (MGB™) probes to distinguish SNPs (3, 65, 90). Primers and probes (Table 2.1) were designed using Primer Express Software, Version 2.0 (Applied Biosystems). Primers were obtained from Qiagen. Fluorescent MGB™ probes were produced by Applied Biosystems and labeled with reporter dyes, 6FAM or VIC, at their 5' ends and non-fluorescent quencher molecules at their 3' ends. Primer and probe concentrations were optimized according to the TaqMan Universal PCR

Master Mix technical bulletin (Applied Biosystems) using DNA obtained from *P. falciparum* strain 3D7 or from patient specimens. 300 nM of both forward and reverse primers were found to be optimal for all SNPs. Optimal probe concentration was determined to be 250 nM for all MGB probes used in this study. Using 10-fold serial dilutions of 3D7 genomic *P. falciparum* DNA, as few as 8 copies (0.001 ng) of genomic *P. falciparum* DNA could be detected.

Each real-time PCR amplification reaction contained both the wild type probe labeled with FAM, and the mutant probe labeled with VIC. Presence of either SNP could be imputed from the relative increase of fluorescence of the two fluorophores (Figure 2.2). Mixed infections were detected by the increase of fluorescence from both flurophores. All reactions were done in duplicate.

Parasite culture

Of the 74 patients enrolled, parasites were successfully cultured from 59. Following treatment, 20 of the 74 admission patients recrudesced. Parasites were successfully cultured from 13 of these 20 recrudescent patients (Figure 2.1).

Results

Real-Time PCR is sensitive and specific

The sensitivity and specificity of SNP detection using real-time PCR were measured in 22 post-culture DNA samples using DNA sequencing as the gold standard (Table 2.2). Nineteen cultures were derived from blood of patients upon admission to the study. The other three cultures were obtained from those who failed treatment. Two samples contained mixtures of SNPs at single positions based on DNA sequencing. Of the 20 monoclonal samples, 19 were concordant for all *pfmdr1* SNPs when analyzed using both methods. The discordant sample

was not an artifact since both the real-time PCR and sequencing reactions gave identical results when repeated. The discordant sample contained a single discrepancy at position 184 (phenylalanine by sequencing and tyrosine by real-time PCR). Thus, the sensitivity of real-time PCR method to detect Tyr^{86} or Asp^{1042} SNPs was 100% and the sensitivity to detect Phe^{184} was 92%; there were no Cys^{1034} mutations detected. Real-time PCR was 100% specific for each mutation. The sensitivity and specificity of the assay to detect all four SNPs were 94% and 100%, respectively.

Two of the 22 samples were found to be mixed infections when sequenced. One sample contained a mixture of Tyr^{184} and Phe^{184}. The other sample contained a mixture of Asn^{86} and His^{86}. The real-time PCR method accurately identified the Tyr^{184}/Phe^{184} mixed population. However, because the probes were designed to detect only Asn^{86} or Tyr^{86}, His^{86} was not detected by real-time PCR.

Comparison of SNPs in paired pre- and post-culture DNA

In order to determine how the process of culturing parasites in vitro alters genotype, a comparison was made between the *pfmdr1* genotypes of DNA extracted from pre-and post-culture parasites as measured by real-time PCR. Of the paired pre- and post-culture specimens, both members of 68 pairs were successfully amplified by real-time PCR. Fifty-eight of these pairs were obtained from admission patient blood while 10 pairs were derived from recrudescent patients.

Fifty-eight of the pre-culture genotypes were monoclonal, nine pre-culture samples had mixtures of alleles at single positions, and one had mixed SNPs at two positions (184 and 1042). Table 2.3 shows the number of isolates with specific combinations of *pfmdr1* genotypes pre- and post-culture at each specific locus. Isolates with identical genotype at

each locus before and after culture are enumerated in the shaded diagonal. Overall, 54 of 68 (79%) pre-culture DNA samples were completely concordant with post-culture DNA at all four polymorphic sites examined. While there was a wide variation in the length of time parasites were cultured before DNA was extracted, there was no correlation between genotype discordances and length of time in culture (data not shown). Five of the 14 discordant isolates exhibited single differences at position 184, and two were different at position 1042. Seven discrepant samples contained mixtures of alleles at one or more sites before and/or after culture. Six samples showed a mixture of alleles pre-culture and single alleles post-culture. This type of selection occurred at amino acid 184 for four isolates, and 1042 for two isolates. Two of these six also had changes at a second position, amino acid 86. Finally, one of the seven samples was monoclonal at amino acid 184 pre-culture but polyclonal post-culture (and also exhibited a change from Asn to Asp at 1042).

There was no correlation between discordant samples and selection for the mutant genotypes associated with the drug resistant phenotype. Seven of the 14 discordant samples resulted in the wild type genotypes after isolates were cultures. The remaining 7 discordant isolates contained mutant genotypes following culture.

Novel His86 mutation identified

In one DNA culture sample neither wild type nor mutant probes revealed amplification during real-time PCR. This post-culture sample was amplified by standard PCR methods and sequenced to genotype the position 86 region. Sequencing this sample revealed a His^{86}.

Discussion

In this paper, a real-time PCR method is described which accurately ascertains parasite *pfmdr1* genotype. This method has high sensitivity (94%) and specificity (100%) for

detecting four *pfmdr1* SNPs associated with drug resistance. There was 21% discordance in the real-time PCR genotype results between DNA samples obtained directly from patient blood and DNA samples obtained from subsequent *in vitro* cultures.

Real-time PCR offers several advantages over standard PCR methods for genotyping DNA. First, because of the small sample volume, costs for real-time PCR are much lower than for standard PCR. Second, using real-time PCR, a single technician can perform and analyze hundreds of reactions per day, thus reducing the labor cost as well. Third, this method reduces the opportunity for post-PCR contamination. Once the sample is prepared with the reagents, amplification and analysis are completed in a closed-tube system. Finally, real-time PCR analysis of genotype is easier and requires less scientific expertise for analysis. Thus, the initial cost of a real-time PCR instrument (~$40,000) would be offset by savings in labor, quality assurance, and materials in labs analyzing large numbers of samples.

In this paper, a novel 86^{His} mutation was identified in one post-culture DNA sample. To our knowledge, this mutation has never been identified before and may or may not be associated with drug resistance. Further studies on this mutation are needed to determine if this mutation exists in additional parasite DNA samples using a probe specific for the 86^{His} mutation. In this instance, the mutation may have been selected for when parasites were cultured and was not correlated with recrudescence.

A previous study utilized a novel real-time PCR technology to identify *pfmdr1* SNPs in parasite DNA extracted from clinical blood samples (39). Although the chemistry of the assay differed from the technique described here, both studies yielded similar results and concluded that real-time PCR may accurately detect $Asn^{86} \rightarrow Tyr^{86}$, $Tyr^{184} \rightarrow Phe^{184}$, $Ser^{1034} \rightarrow Cys^{1034}$ and $Asn^{1042} \rightarrow Asp^{1042}$ in *pfmdr1*. In addition, de Monbrison, et al., used this

method to genotype $Asp^{1246} \rightarrow Tyr^{1246}$. SNPs at 1246 were not studied here because they have not been found in South-east Asia (114, 118).

Twenty-one percent of samples manifested differences in *pfmdr1* genotype pre- and post-culture. Since most patients are probably infected with a mixture of strains, the genotypes observed post-culture reflects the results of the selection of a subset of strains by in vitro culture conditions. This could manifest itself as loss of strains observed pre-culture or the appearance of strains not observed pre-culture because they were present at levels below detection limits. A much greater change in genotype (74.5%) was observed in a previous study looking at variations in the polymorphic regions of *merozoite surface protein 1* and *merozoite surface protein 2* as well as GLURP (glutamate-rich protein) (159), perhaps because these genes are more variable.

In addition to SNP detection, our group has previously described a real-time PCR method to measure *pfmdr1* gene amplification (114). Thus it is now possible to assess both *pfmdr1* gene copy number and SNPs using real-time PCR making it possible to carry out a complete assessment of *pfmdr1* genetics in large cohorts.

In conclusion, real-time PCR is a sensitive and specific method to detect *pfmdr1* mutations associated with antimalarial drug resistance directly from patient blood. Our studies suggest genotypic changes occur when patient isolates are cultured. The resulting genotype is not necessarily reflective of parasite populations in vivo and drug sensitivity determined from parasites following a period of in vitro culture should be evaluated with caution. Because it is inexpensive and amenable to high-throughput, it could be a useful public health tool for drug resistance surveillance and to predict treatment failure in patients.

Figure 2.1: Schematic representation showing sources of samples used in study. Of all the samples that amplified with real time PCR, we had 68 pairs of pre- and post-culture DNA

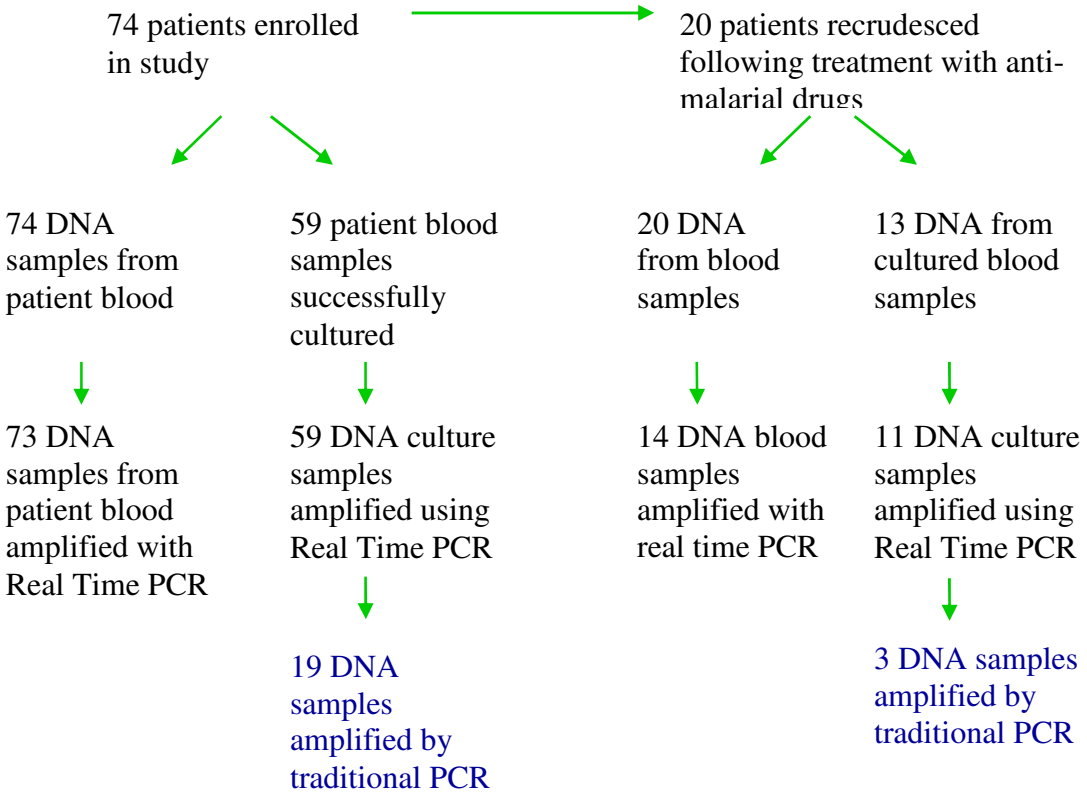

.

Table 2.1: Primers and probes used in real time PCR assay

Pfmdr1		Oligonucleotide (5'-->3')	Tm***
86	F	TGTATGTGCTGTATTATCAGGAGGAAC	63.1
	R	AATTGTACTAAACCTATAGATACTAATGATAATATTATAGG	61.7
	Asn (wt*) probe	6FAM-ACCTAAAT**T**CATGTTCTTT-MGB-NFQ	66.5
	Tyr (mut**) probe	VIC-ACCTAAAT**A**CATGTTCTTT-MGB-NFQ	65.8
184	F	AAGATGGACAATTTCATGATAATAATCCT	59
	R	AATACATAAAGTCAAACGTGCATTTTTTA	57.6
	Tyr (wt) probe	6FAM-CTTTTTAGGTTTAT**A**TATTTGGT-MGB-NFQ	65.2
	Phe (mut) probe	VIC-CTTTTTAGGTTTAT**T**TATTTGGT-MGB-NFQ	65.9
1034	F	AAAAAGAAGAATTATTGTAAATGCAGCTT	57.6
	R	GGATCCAAACCAATAGGCAAAA	58.9
	Ser (wt) probe	6FAM-ATTC**A**GTCAAAGCGCT-MGB-NFQ	65.8
	Cys (mut) probe	VIC-ATTC**T**GTCAAAGCGCT-MGB-NFQ	66.7
1042	F	AAAAAGAAGAATTATTGTAAATGCAGCTT	57.6
	R	TTTCCAGCATAACTACCAGTAAATATAAAAG	60.7
	Asn (wt) probe	6FAM-CAATTATTTATT**A**ATAGTTTTGC-MGB-NFQ	65.3
	Asp (mut) probe	VIC-AATTATTTATT**G**ATAGTTTTGC-MGB-NFQ	64.8

* Wild type (Asn86, Tyr184, Ser1034 or Asn1042) sequence

** Mutant (Tyr86, Phe184, Cys1034 or Asp1042) sequence

*** Melting temperature estimated by Primer Express v2.0

For probes, the reporter dye is covalently attached at the 5'end (6FAM or VIC) with a minor groove binder (MGB) and non-fluorescent quencher (NFQ) covalently attached at the 3' end.

Figure 2.2: Fluorescence intensity (Rn) of the FAM reporter dye (blue line) compared to VIC reporter dye (green line) as PCR amplification cycles proceed (x axes).

Fluorescent intensity is measured as Rn (y-axes), the absolute fluorescence of the reporter dye divided by that of the passive reference dye, Rox. An increase in FAM indicates a wild type population [86(e), 184(f), 1034(g), 1042(h)] while an increase in VIC indicates a mutant population [86(a), 184(b), 1034(c), 1042(d)]. Mixed infections may be identified by an increase in fluorescent intensity of both reporter dyes (not shown). Mutant 1034 DNA (c) was obtained from a previous study (114) because none of the samples in this study contained that mutation.

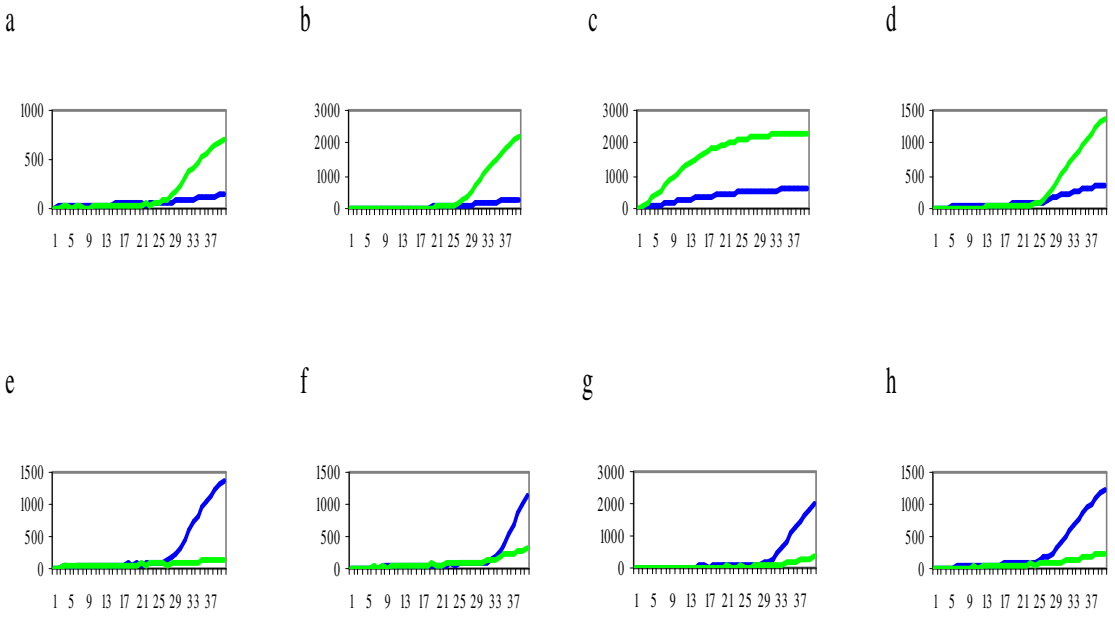

Table 2.2: Prevalence of mutations in monoclonal culture samples (n=20) of mutations detected by traditional PCR and sequencing (gold standard) and real-time PCR, and sensitivity and specificity of real-time PCR assay.

	Prevalence		Real Time PCR	
	PCR	Real Time PCR	Sensitivity	Specificity
Tyr86	5%	5%	1/1 (100%)	19/19 (100%)
Phe184	65%	60%	12/13 (92%)	7/7 (100%)
Cys1034	0%	0%	0/0 (--)	20/20 (100%)
Asp1042	10%	10%	2/2 (100%)	18/18 (100%)
All mutations correct	--	--	15/16 (94%)	64/64 (100%)

Table 2.3: Genotype results of pre-culture and post-culture DNA by real time PCR

			Post-Culture Genotype Results								
	Codon		86			184			1042		
		Amino Acid	Asn	Tyr	His	Tyr	Tyr & Phe	Phe	Asn	Asn & Asp	Asp
Pre-Culture Genotype Results	86	Asn	64	--	*1						
		Tyr	1	2	--						
		His	---	--	--						
	184	Tyr				27	1	2			
		Tyr & Phe				2	4	2			
		Phe				3	--	27			
	1042	Asn							60	--	3
		Asn & Asp							1	--	1
		Asp							--	--	3

* Result from standard PCR and sequencing following inconclusive real time PCR results
Data for codon 1034 was omitted because no mutant or polyclonal infections were detected in the 68 paired samples.

Table 2.4: Prevalence of mutations in patient blood (gold standard) and post-culture samples and sensitivity and specificity of PCR on culture-derived parasites.

	Prevalence[a]		Culture	
Genotype	Blood[b]	Culture[c]	Sensitivity	Specificity
Tyr^{86}	4	2	2/3 (67%)	65/65 (100%)
Phe^{184}	56	53	33/38 (87%)	27/30 (90%)
Cys^{1034}	0	0	0/0 (--)	68/68 (100%)
Asp^{1042}	7	10	4/5 (80%)	60/63 (95%)
1 mutation per sample[d]	53	47	--	--
2 mutations per sample[e]	7	10	--	--
All mutations correct	--	--	39/46 (85%)	225/231 (97%)

Note
n=68
[a] displayed as percentage
[b] pre-culture DNA
[c] post-culture DNA
[d] mutations found at a single codon position
[e]mutations found at multiple codon positions

CHAPTER 3

Target and Mechanism of Action for [2,5-bis(4-amidinophenyl)furan] in *Plasmodium falciparum*

PREFACE

The following chapter is in preparation for publication. Contributing authors include: Anne Purfield, Richard R. Tidwell and Steven R. Meshnick. Anne Purfield is the primary author and has designed and conducted all experiments including subcellular localization with confocal microscopy, stage specificity and real time PCR analysis of gene expression. Michael Chua of the Michael Hooker Microscopy Facility captured the confocal images and Jaina Patel assisted with parasite maintenance and calculating parasitemias for the gene expression assays.

This research was supported by Medicines for Malaria Venture and the Bill and Melinda Gates Foundation.

CHAPTER 3

Target and Mechanism of Action for DB75, [2,5-bis(4-amidinophenyl)furan], in *Plasmodium falciparum*

Introduction

Resistance to classical antimalarials exists throughout the developing world (172). Most of the current antimalarials belong to a few classes of compounds for which cross-resistance exists. New antimalarials with unique targets are needed to overcome cross resistance.

Pentamidine, [1,5-di(4-amidinophenoxy)pentane], a dicationic diamidine, has been used for clinical treatment of protozoan infections such as leishmaniasis and Human African trypanosomiasis (HAT) (165). It also has activity against *Plasmodium falciparum*; however, the drug is not orally bioavailable and has considerable side effects, including renal toxicity and cardiotoxicity (5, 21, 52). Therefore, it has been passed over as a potential malaria therapeutic in favor of drugs with oral bioavailability and fewer side effects (21). New pentamidine structural analogues under consideration as an alternative treatment for HAT represent a class of broad-spectrum antimicrobials with orally active prodrugs lacking the side effects associated with pentamidine (13, 122). The aromatic diamidines inspired by pentamidine are being investigated for therapeutic use with HAT, malaria, *Pneumocystis jiroveci* pneumonia (PCP) and leishmaniasis (13, 165).

The dicationic diamidine, DB75, [2,5-bis(4-amidinophenyl)furan], is a structural analogue of pentamidine with antimicrobial activity, but it lacks oral bioavailability (11, 13, 19). DB289, [2,5-bis(4-amidinophenyl)furan *bis*-*O*-methylamidoxime], is the orally active pro-drug of DB75 (18, 122, 178). In a clinical trial of Thai patients with falciparum malaria, DB289 monotherapy (100mg, twice daily for 5 days) exhibited a 96% (22 of 23) cure rate (178). In addition to its activity against Plasmodium species, DB289 is active against early

stage HAT and PCP, and it is currently in Phase III clinical trials for treatment of these infections (personal communication, Richard R. Tidwell).

The target and mechanism of action of diamidines against malaria are currently unknown but several possible mechanisms have been proposed. First, Stead et al. showed that pentamidine is found in the food vacuole of *P. falciparum* where it binds toxic heme and inhibits formation of non-toxic hemozoin (147). Second, DNA-containing organelles are also potential targets. In *Trypanosoma brucei gambiense*, DB75 localizes in DNA-containing organelles, such as the nucleus and kinetoplast (86, 97). Further, nucleic acid-binding is believed to inhibit topoisomerase II, a DNA replication enzyme, in *Giardia lamblia* (11, 96). Also, DB75 inhibits cellular respiration in the mitochondria of *Sacchharomyces cerevisiae* and trypanosomes (personal communication, Charlotte A. Lanteri, (86)) Finally, DB75 localizes in acidocalcisomes of trypanosomes where it may interrupt calcium homeostasis (97). Plasmodium also possess acidocalcisomes that regulate calcium homeostasis in a manner similar to other protozoan (92).

The objective of this investigation is to elucidate the mechanism of action for DB75 in *P. falciparum*. We used fluorescence co-localization to demonstrate DB75 subcellular localization in the nucleus. In addition we showed that the drug exhibits stage-specific killing action in which ring stage parasites are more sensitive than trophozoites and development is delayed with DB75 exposure. Finally, we determined the effects of DB75 on the expression of six developmentally regulated genes throughout the life cycle.

Materials and Methods

Parasite cultivation

3D7 *P. falciparum* strain was maintained with 2% (v/v) O^+ human erythrocytes (Research Blood Concepts, Brighton, MA) in 1640 RPMI supplemented with 25mM HEPES (Sigma), 2mM L-glutamine (Gibco), 0.45% (w/v) glucose (Sigma), 0.05ng/ml gentamycin (Sigma), 0.1 mM hypoxanthine and 10% (v/v) O^+ human serum (Research Blood Concepts). Cultures were maintained by the Trager and Jensen method in candle jars with low oxygen tension and incubated at 37^{o}C (155).

[^{3}H]-Hypoxanthine Incorporation Assay

We measured [^{3}H]-hypoxanthine incorporation into parasite DNA in the presence and absence of DB75 to assess parasite drug susceptibility in vitro. (41). Parasite cultures were diluted to 0.7% parasitemia (percent infected red blood cells) in complete medium (without supplemental hypoxanthine). Parasites were sub-cultured in 96-well flat bottom microtitre plates with serial dilutions of DB75 at final concentrations ranging from 1μM to 3.9nM.

To measure growth in 42 hours, the 96-well plates were incubated for 24 hours prior to addition of 0.5μCi of [^{3}H]-hypoxanthine diluted in hypoxanthine-free complete media (25μl/well). The cells were incubated for an additional 18 hours and harvested using an Inotech cell harvester and glass fiber filter paper (Inotech Systems International, INC.). Radioactivity of samples was determined in a liquid scintillation counter (Beckman-Coulter) (41). Background absorption of [^{3}H]-hypoxanthine by erythrocytes was controlled for using uninfected erythrocytes, and maximum parasite growth was controlled for using nontreated parasites.

DB75 concentration required to inhibit 50% of parasite growth (IC50) was calculated using sigmoidal dose response nonlinear regression equation in GraphPad Prism® (version 4.0).

Confocal microscopy

Asynchronous parasite-infected red blood cells were stained with fluorescent dyes for subcellular localization studies. Cells were treated with MitoTracker Red CMXRos (Invitrogen) which is a mitochondrion-specific dye or LysoTracker® Red DND-99 (Invitrogen), an acidophilic dye that localizes to the parasite food vacuole (74, 139). Cells were also treated with Draq5™ (Axxora, LLC), a nuclear DNA dye in addition to the inherently fluorescent compound, DB75 (Table 3.1) (95).

To determine if DB75 co-localizes with MitoTracker Red, red blood cells infected with viable asynchronous parasites suspended in medium were incubated with 25nM MitoTracker Red for 30 minutes at 37^{o}C in a candle jar. The cells were centrifuged and resuspended in pre-warmed complete medium to remove the mitochondrial dye from the extracellular medium. 1μM DB75 was added and cells were transported to the Michael Hooker Microscopy facility (15 minutes) where 1μM of the DNA dye was added immediately prior to slide preparation. To determine if DB75 co-localizes with LysoTracker Red, infected red blood cells were prepared as described above except cells were incubated with 50nM of LysoTracker.

To assess DB75 co-localization with Draq5™, 1μM DB75 was added to infected red blood cells suspended in medium prior to transport to the microscopy location. 1μM of the nuclear dye was added immediately prior to slide preparation.

To determine subcellular localization with short-term drug exposure, infected red blood cells (>5% parasitemia) were incubated with 1μM DB75 for less than four hours prior to microscopy. For long term drug exposure, infected red blood cells (3% parasitemia) were exposed to 100nM DB75 for 24, 48 or 72 hours. Dyes for co-localization with DB75 were

added after the long exposure periods to determine the subcellular localization of the drug. To determine if DB75 remains in the parasite after extracellular drug pressure is relieved, parasites were exposed to DB75 for 24 hours and then washed by centrifugation and resuspended in drug-free pre-warmed medium. The parasites were incubated for an additional 48 hours prior to microscopy.

For confocal microscopy, live cells were examined under a cover slip using a Leica 2SP Laser Scanning Confocal Microscope. The 561nm Solid State laser was used to capture MitoTracker (absorbance/emission: 579nm/599nm) or LysoTracker (absorbance/emission: 577nm/590nm); a UV laser (364nm) for DB75 (absorbance/emission 365nm/465nm) and Red HeNe laser to capture Draq5™ (absorbance/emission: 647nm/670nm) (Table 3.1). A spectral scan was used to identify changes in the emission spectrum of DB75. Adobe Photoshop (v.7.0) was used to create overlaid confocal images and to adjust dye contrast for publication.

Parasite maturation assay

To determine the effect of DB75 on parasite maturation, parasites were synchronized at the ring stage with 5% sorbitol for 10 minutes, followed by 3 washes in RPMI medium (84). Cultures were synchronized every 48 hours for 3 consecutive life cycles prior to a 24-48 hour recovery period. Infected red blood cells with synchronized ring or trophozoite parasites (0.3% parasitemia) were exposed to DB75 for 96 hours. Medium for each sample was exchanged at 48 hours with fresh medium and DB75. Nontreated synchronized cultures were used as a control. Thin blood smears were prepared and stained with Giemsa stain at 0, 12, 24, 36, 48, 60, 72, 84 and 96 hours post-exposure and examined with light microscopy to assess parasitemia and parasite morphology. Parasitemia was determined by calculating the

number of parasite-infected red blood cells per at least 1000 total red blood cells. Parasite morphology was examined and the number of rings, trophozoites and schizonts was assessed for at least 100 parasites. Parasites with the "ring" structure and a single nucleus were classified as ring stage parasites. Parasites containing a single nucleus and hemozoin were classified as trophozoites. Multi-nucleated parasites with ample hemozoin were classified as schizonts.

Gene expression

Red blood cells infected with sorbitol-synchronized rings were exposed to 100nM or 500nM DB75 for 48 hours. Nontreated cells were used as a control. At 0, 6, 12, 18, 24, 36 and 48 hours, RNA and DNA were immediately extracted from the harvested cells using the Allprep kit (Qiagen). Also, blood smears were prepared for assessment of morphology and parasitemia at each time point. RNA concentrations were measured using a NanoDrop 1000 (NanoDrop Technologies). 50ng of total RNA was reverse transcribed using SuperScript® II (Invitrogen) with 2.2μM $Pd(N)_6$ Random Hexamer (GE Healthcare) and 2.2μM Oligo(dT)20 primers (Invitrogen) according to the manufacturer's protocols. All cDNA samples were diluted by a factor of 50 in sterile, RNase free water, and 5μL was subsequently used for Real Time PCR to measure expression in six developmentally-regulated genes. Primers were designed using Primer Express v3.0 (Applied Biosystems) (Table 3.2).

Real Time PCR was performed using an Applied Biosystems 7300 Real-Time PCR System (Applied Biosystems) with Power SYBR® Green PCR Master Mix (Applied Biosystems). cDNA was amplified with 40 cycles of: 95^{o} for 15", 55^{o} for 30", 72^{o} for 30". A dissociation curve for amplicon melting temperature analysis was performed immediately

following amplification to monitor nonspecific amplification (contamination or primer dimer amplification).

The expression of each gene relative to a constitutively expressed gene was analyzed for each sample (113). Expression of six developmentally expressed genes were assessed: *trophozoite antigen R45-like* (ring stage), *lactate dehydrogenase* (late ring stage), *DNA primase* (trophozoite stage), *isocitrate dehydrogenase* (trophozoite stage), *merozoite surface protein-1* (schizont stage), *merozoite surface protein-7* (schizont stage) (Table 3.2) (20). In replicates on the same reaction plate, amplification of cDNA for a developmentally-regulated gene was compared to that of the constitutively expressed, 18s rRNA. The amplification efficiency for each primer pair was calculated based on the slope of the line representing cycle threshold (CT) values versus 3D7 genomic DNA concentrations from five separate experiments as previously described (113). To determine the relative fold change in expression over time for each developmentally-regulated gene, we used the following equation (113):

$$\text{Fold Change in Gene Expression} == \frac{(E_i)^{\wedge}(CT_{i,t} - CT_{i,t=0})}{(E_{ref})^{\wedge}(CT_{ref,\,t} - CT_{ref,\,t=0})}$$

Where E is primer efficiency, CT is the cycle threshold, *i* is the developmentally-regulated gene of interest, *t* is the time of drug exposure, *t=0* is the start of the experiment and *ref* is the 18s rRNA reference gene (113). This method accounts for variations in cDNA concentrations and differences in primer efficiency. Data were graphed using GraphPad Prism® (v.4.03). Results are representative of 2 separate experiments.

Results

DB75 inhibits P. falciparum growth

To determine the antimalarial activity of DB75 in vitro, we measured tritiated hypoxanthine incorporation. DB75 exhibits mean±SEM IC50 values of 124nM±10 with asynchronous parasites exposed for 42 hours (Figure 3.1). When synchronized ring and trophozoite cultures were exposed to DB75 for 36 hours, the mean±SEM IC50 for rings was 143±8 compared to 711±32 for exposed trophozoites, suggesting DB75 has stage specific activity where rings are more sensitive (Figure 3.1). The mean±SEM IC50 was reduced to 1.5nM±0.2 for synchronized rings exposed for 96 hours, suggesting longer incubations increase DB75 inhibitory activity (Figure 3.1).

Fluorescent localization of DB75 in P. falciparum

We utilized the intrinsic fluorescent properties of DB75 to determine its potential subcellular localization in *P. falciparum* using confocal microscopy. To identify possible sub-cellular targets, we incubated infected red blood cells with DB75 and different organelle-specific dyes as described in the methods (74, 95, 139). In parasites exposed to 100nM or up to 1μM drug for less than four hours, DB75 co-localized only with Draq5™, the nuclear DNA stain. Nuclear co-localization was evident in all parasite life stages except the ring stage with short-term exposure (Figure 3.2), suggesting that the drug initially localizes in the nucleus and may require a stage-specific uptake mechanism that prevents accumulation in ring stage parasites. DB75 had a distinct and separate staining pattern from the red-fluorescing LysoTracker or MitoTracker, suggesting that DB75 does not co-localize with these dyes in the food vacuole or mitochondrion immediately after drug exposure. 3-D

compilations of z-series images confirmed DB75 co-localized only with Draq5™ and not LysoTracker or MitoTracker (data not shown).

To determine if DB75 localizes to other subcellular compartments over time, asynchronous parasites were exposed to a therapeutic concentration (100nM) of DB75 for 24, 48 or 72 hours. Despite the longer incubation, DB75 co-localized only with Draq5™ following 24, 48 or 72 hours, suggesting the drug targets the nucleus of the parasites with extended exposures (Figure 3.3). DB75 co-localization with Draq5™ was noted in all life stages after 24 hours of exposure, including rings. Although DB75 was not evident in ring stage parasites with short-term drug exposure, the presence of DB75 in rings after extended drug exposure suggests DB75 may not be transported into the cell during the early part of the life stage. However, with extended exposure DB75 localization in the nucleus of schizonts likely persists as the host cell ruptures and merozoites invade uninfected erythrocytes and mature to the ring stage.

After 48 or 72 hours of continuous exposure of infected red blood cells to 100nM DB75, the drug's emission spectrum undergoes a shift from 465nm (blue) to 558nm (yellow), although still localized to the nucleus (Figure 3.4). This spectral shift may be the result of high concentrations of the compound, as is seen with the DNA-binding dye, Hoechst (112). A similar shift from blue to yellow fluorescence is also observed by epifluorescence in trypanosomes exposed to 7.5μM DB75 (97).

To determine if and where DB75 persists in the cell after drug pressure was removed, live cells were assessed with co-localization dyes 48 hours after drug was removed. When *P. falciparum* cells were washed after 24 hours of continuous exposure to 100nM DB75, the blue DB75 fluorescence was still observed in the nucleus of cells at 48 and 72 hours post-

exposure by colocalization with Draq5™. However, only the blue fluorescence (465nm emission) was detected (Figure 3.3). This suggests that the drug remains in the nucleus, perhaps bound to DNA, but does not accumulate to high levels that may result in the fluorescence shift from blue to yellow.

With 72 hours of continuous DB75 exposure, the nontreated control parasites were healthy at all life stages observed by both confocal and light microscopy (data not shown). However, all DB75-treated parasites appeared to be unhealthy or dead following 72 hours of continuous exposure to 100nM DB75 (Figure 3.4). Many treated parasites were outside of the host red blood cells, and all exhibited condensed nuclei. Extracellular and pycnotic parasites were also observed by light microscopy using Giemsa stained blood smears (data not shown).

DB75 is stage specific

To determine the stage-specific effect of DB75 on parasite maturation and morphology, we examined parasite growth and morphological changes over two full life cycles when either ring or trophozoites were initially exposed to drug. Parasite maturation and survival time was dependent on parasite life stages at the time of initial exposure; rings were more sensitive to DB75 than trophozoites. This observation was consistent with growth assays using synchronized infected red blood cells (Figure 3.1).

Our results show that nontreated cells progressed through the 48-hour life cycle as expected (Figure 3.5a and c). When exposed to DB75 as rings, the parasites matured with the trophozoite population peaking at 24 hours after exposure (Figure 3.5a). A subsequent population of schizonts peaked at 36 hours and is followed by an increase in parasitemia and a new ring population, initiating the second life cycle. The ring population peaked at 60

hours post-exposure, followed by a trophozoite population at 72 hours and schizonts at 96 hours.

Like the nontreated rings, the nontreated trophozoites also progressed through two life cycles as expected (Figure 3.5c). In completion of the initial life cycle, the trophozoite population progressed to schizonts, which peaked at 12 hours. The schizonts ruptured, increasing the parasitemia and initiating another life cycle with the first ring population. The ring population peaked at 24 hours, and progressed to trophozoites which peaked at 48 hours. The schizont population peaked shortly thereafter at 60 hours, and in the next life cycle the parasitemia rose again with the appearance of a second ring population. The second ring population peaked at 84 hours and progressed to trophozoites then schizonts by 96 hours.

However, when parasite-infected red blood cells were exposed to DB75 for 96 hours, a stage-specific delay in maturation was observed. In both exposed rings and trophozoites, there was no change in the timing of the first ring populations compared to nontreated cells (Figures 3.5). In exposed rings, the first ring population persisted until 24 hours (Figure 3.5b); and in exposed trophozoites, the first ring population appeared at 24 hours after exposure (Figure 3.5d). However, there were differences in the first trophozoite population. In treated exposed rings, the trophozoites peaked at 24 hours (same as nontreated cells), but the population persisted with a slow decline, suggesting the parasite maturation was delayed at this stage (Figures 3.5a and b). In treated exposed trophozoites, the fist trophozoite population is almost identical to that of the nontreated trophozoites (Figures 3.5c and d).

The delayed maturation was also evident in the first schizont populations of DB75-exposed ring- and trophozoite-infected red blood cells. In treated exposed rings, the first schizont population was diminished and peaked at 48 hours instead of 36 (Figure 3.b). The

inhibition and delay were absent in exposed trophozoites for the first schizont population peaks at 12 hours for both treated and nontreated cells (Figure 3.5d).

The appearance of the second ring population in both drug-exposed ring- and trophozoite-infected red blood cells was practically absent, suggesting the drug prevents the initiation of a second complete life cycle. This is evident by the parasitemia, which did not increase after the first ring population is exposed to drug (Figure 3.5b), further suggesting the parasites must be exposed to DB75 during the ring stage for delayed maturation during the trophozoite stage. Consequently, the second trophozoite population in exposed trophozoite-infected red blood cells peaked 12 hours after the nontreated cells, and exhibited a slow progression to schizonts as observed with the first trophozoite population in exposed rings (Figure 3.5d). Taken together, these results suggest ring-stage parasites are more sensitive than trophozoites and a stall in maturation occurs after the first ring population is exposed to DB75.

To determine if the inhibitory effects of DB75 were reversible, infected red blood cells were exposed to drug for 48 hours, and then the drug was removed by washing, and cells were incubated for an additional 48 hours without drug. For infected red blood cells exposed to 100nM DB75, parasitemia levels did not increase during the 48 hours after DB75 was removed (Figure 3.7). At 48 hours the parasitemia±SD for 100nM treated rings was 0.13±0.6%. 48 hours after drug pressure was removed, the parasitemia±SD was 0.10±0%. Rings exposed for 96 hours exhibited a similar growth pattern as the cells with drug removed (Figures 3.6a and 3.7a). Removal of drug at 48 hours also had no effect on the sensitivity (Figures 3.6b and 3.7b). These data suggest that the inhibitory effects of DB75 are irreversible after 48 hours.

DB75 effect on gene transcription

We measured the effect of drug on transcription for six developmentally regulated genes (Table 3.2) (20). With synchronized ring-stage parasites, we assessed the transcription profiles for alterations in genes expressed during specific life stages relative to a constitutively-expressed gene.

For genes normally expressed during the early life stages, *trophozoite antigen R45-like* and *lactate dehydrogenase*, peak expression occurred in the first 12 hours following invasion for untreated rings (Figure 3.8a). A similar pattern was observed for cells exposed to 100nM or 500nM DB75 (peak expression, 12 hours). The fold change in expression (peak intensity) relative to 18s rRNA for these early transcribed genes varied little with DB75 exposure. The peak intensity in nontreated cells was 2.0 for *lactate dehydrogenase* and 2.2 or 1.7 with addition of 100nM or 500nM DB75, respectively (Figure 3.8b). Similarly, peak intensity for *trophozoite antigen R45-like* was 1.0 for both nontreated and treated cells. The DB75 treatment had little or no effect on the timing or intensity of expression of these early genes.

The effects of DB75 were also measured for two trophozoite-specific transcripts: *isocitrate dehydrogenase* or *DNA primase*. Peak expression for these genes in untreated rings occurred later than expected at 36 and 48 hours, respectively (Figure 3.8a). Unlike the ring-stage genes, peak expression for the trophozoite-specific transcripts was altered with addition of drug. With 100nM DB75, the expression of *isocitrate dehydrogenase* occurred in exposed rings at 30 hours post-invasion which is 6 hours earlier than nontreated cells (Figure 3.8a). The highest concentration of DB75 had the opposite effect. Peak expression was delayed 6 hours to 42 hours post-invasion. 500nM DB75 also delayed expression of *DNA primase* by 12 hours relative to nontreated cells (60 hours). The delays observed with the highest concentration of DB75 were consistent with the delay in maturation.

The intensity of peak expression for both *isocitrate dehydrogenase* and *DNA primase* with 500nM DB75 was increased (Figure 3.8b). This is especially evident for DNA primase where there was a 61-fold increase in expression in nontreated cells but 192-fold increase with addition of 500nM DB75. A similar trend was observed with exposure to 5nM atovaquone (data not shown), suggesting that the increased *DNA primase* expression may be a nonspecific response to drug or cell death rather than a specific response to DB75. The lower concentration of DB75 did not have a pronounced effect on peak intensity for either *isocitrate dehydrogenase* or *DNA primase* (57-fold) compared to non-treated cells (Figure 3.8b). Thus, the expression of the trophozoite-stage genes are both delayed and increased by 500nM drug.

We also measured the effect of drug on genes expressed during the schizont stage, *merozoite surface protein-1* and *merozoite surface protein-7*. For nontreated ring stage cells, peak expression occurred at 48 hours post invasion, when parasites were at the schizont stage. There was no change in *merozoite surface protein-7* peak expression time with 100nM DB75 (48 hours) (Figure 3.8a). However, the same concentration of DB75 delayed peak expression of *merozoite surface protein-1*. Additionally, 500nM DB75 delayed the expression of both schizont-stage genes by 6 or 12 hours. Also, 500nM DB75 drastically reduced peak intensity of these late-stage genes. *Merozoite surface protein-1* expression was reduced from a 139-fold increase to 0.7 (Figure 3.8c). *Merozoite surface protein-7* peak expression intensity was reduced from a 6.8 fold increase to 1.1. Again, this is consistent with the delayed maturation effect observed above.

We also determined the effect on developmental gene expression using DB75-exposed synchronized trophozoites (data not shown). Similar to exposed-rings, the expression of

mid- and late-stage expressed genes was delayed with 500nM DB75. The exception to this was *isocitrate dehydrogenase*, for which peak expression was 36 hours post-invasion for both DB75-treated and untreated cells. Unlike like the drug-exposed rings, peak intensity for late-stage genes, *merozoite surface protein-1* and *merozoite surface protein-7*, was not diminished but similar to nontreated parasites. However, peak intensity of *DNA primase* was increased from 39-fold in nontreated cells to 171-fold with 500nM DB75.

Taken together, DB75 does not appear to enhance or suppress selected genes whose expression is associated with specific lifecycle stages. However, delays in peak expression for mid- and late-stage expressed genes were observed, and are consistent with the delays observed by microscopy.

Discussion

DB75 is representative of a class of newly synthesized diamidine compounds with antimalarial activity. Confocal microscopy demonstrates that DB75 co-localizes with a nuclear DNA dye in the nucleus after both short (<4 hours) and long exposures (24-72 hours) but not with markers for other organelles, suggesting that DB75 may target the nucleus. The absence of co-localized staining with dyes for the mitochondrion or food vacuole argues against these organelles as targets for DB75; however, due to the complicated nature of fluorescence in the cell, these organelles cannot be completely excluded.

Tritiated hypoxanthine growth assays, in combination with the assessment of morphologies, suggest that ring stage parasites are more sensitive to DB75 than trophozoites, and exposed rings tend to stall in the trophozoite stage. Thus, DB75 may act on the nucleus to affect nucleic acid synthesis or nuclear function occurring during the trophozoite stage. By quantifying transcription of six stage specific genes, we found that DB75 causes delays in

expression but not inhibition of stage-specific transcripts.

Previous reports suggest that the nucleus may be a target for DB75. Epifluorescence and confocal microscopy studies show DB75 localizes to the nucleus and mitochondria of tumor cells (85, 97). Additional studies show DB75 binds to the minor groove of DNA at 5'-AATT-3' (98). Since the nuclear genome of *P. falciparum* is 80% AT rich, we would expect the genome to contain a high number of DB75 binding sites (57). Our results are consistent with these observations and show DB75 selective accumulation in the nucleus of *P. falciparum*.

Our data suggest that DB75 has a different mechanism of action in malaria than in trypanosomes. In trypanosomes, epifluorescence experiments show that DB75 accumulates in the mitochondria, acidocalcisomes, nucleus, and kinetoplast (Charlotte Lanteri, personal communication and (96)). Based on these observations, we expected to see accumulation in the nucleus, mitochondrion and/or acidocalcisomes of Plasmodium. However, our results suggest that subcellular localization of DB75 is limited to the nucleus of the *P. falciparum* parasite. While we cannot eliminate other subcellular targets based solely on DB75 fluorescence, data from Akhil Vaidya's lab are consistent with the observation that DB75 does not affect malarial mitochondria (Akhil Vaidya, personal communication). Further molecular studies may eliminate non-nuclear targets.

Our data are not consistent with the mechanism of action for diamidines proposed by Stead et al., who suggest that diamidine compounds act by targeting the hemozoin synthesis pathway in the food vacuole (147). In solution, 3μM pentamidine binds heme and prevents hemozoin formation as determined by spectroscopy. With confocal microscopy, we show that DB75 does not accumulate in the food vacuole with short term or long term drug

exposure. One possible explanation for this lack of appearance of drug in the food vacuole is fluorescent quenching at low pH. However, DB75 fluorescence is not quenched by low pH (J. Ed Hall, personal communication). Further studies using electron micrographs or isotope-labeled DB75 are needed to definitively rule out the food vacuole as a target.

We report here that DB75 inhibits parasite growth in a stage-specific manner that requires drug exposure during the ring stage. Since DB75 is a DNA-binding compound that localizes in the nucleus, we expected stage-specific inhibition to correlate with nuclear activity, which peaks during the late trophozoite and schizont stages (20, 60, 89). This same apparent paradox was observed for the polymerase-α inhibitor, aphidicolin, which is more effective against ring stage parasites and blocks trophozoite development (70).

We hypothesized that the stage-specific effect of DB75 may be explained, in part, by inhibition of genes transcribed early in the life cycle when DB75 exposure appears to be critical. Stage-specific inhibition is also observed with the antimalarial compound, hexadecyltrimethylammonium bromide, which inhibits late-stage expression of *Plasmodium falciparum choline kinase (pfck)* (28). Late stage parasites are more sensitive to hexadecyltrimethylammonium bromide than early ring stage parasites (28). We expected to see a similar effect with DB75 inhibition of early stage transcripts to explain the stage-specific action of DB75 and increased sensitivity of ring stages. However, our data show that DB75 does not inhibit early stage transcripts at therapeutic concentrations. Since we tested only 6 stage-specific genes, it is possible that DB75 may exert some specific effect on genes not tested. A full microarray analysis may identify such specificity if it exists in *P. falciparum*.

The increased *DNA primase* expression was unexpected. A less pronounced increase was also observed when cells were treated with atovaquone (5nM, data not shown), suggesting the effect may not be drug specific, but a general response to cell death, since atovaquone targets the mitochondria. DNA primase is required for DNA synthesis (26) and further studies are needed to determine how increased *DNA primase* expression is related to the drug mechanism of action. DNA primase translational regulation should also be investigated since DB75 binds to single stranded RNA and could affect post-transcriptional modification or translation (179).

This study has few limitations. First, synchronization of parasites is imperfect. Parasites are synchronized at the ring stage and examination of morphology shows >90% of the parasite population is at the desired state at the start of experiments. The remaining unsynchronized parasites may slightly skew gene expression and morphology results. Second, classification by morphology of parasite life stage is only approximate and imperfect. To minimize this, the samples were blinded to prevent bias and all morphology assessments were determined by one individual. Third, we have shown DB75 localizes in the nucleus, but we cannot definitively say that this is the single target in *P. falciparum*. DB75 may exhibit unknown fluorescent properties, such as quenching, in the presence of biological substrates. Therefore, we cannot conclude that the compound is not present when the fluorescence may, in fact, be quenched. Finally, the complicated nature of capturing images of live parasite-infected erythrocytes with confocal microscopy limited the number of cells we were able to examine.

Taken together, our data suggest a mechanism for DB75 involving nucleic acid synthesis. We propose that the nucleus is the target of DB75. DB75 localizes in the nucleus and slows

the maturation of parasites. This is evident by the stall in development at the trophozoite stage. In addition, DB75 must be present in the early life stages to interrupt nuclear activity in the cell. Inhibition of developmental gene transcription is not likely to be the mechanism of action because alterations with gene expression profiles occur only with the highest concentration of DB75 and appear to be a result of the stall in maturation. However, this study only examined DB75's effect on the transcription of six select genes; future studies should investigate the full extent of the drug's effect on developmental gene expression using microarrays. In addition, the effect of DB75 on DNA synthesis, nuclear enzyme activity and mRNA translation should be examined to further elucidate the mechanism of action. This is the first time the mechanism for antimalarial action of DB75 has been evaluated. Results obtained in this study are potentially relevant to the clinical application of DB289. Also, these results may translate to other dicationic diamidine compounds in development for antimalarial use.

Table 3.1 Subcellular localization dyes used for confocal microscopy

Dye	Target Organelle	Preparation	Absorbance	Emission	Laser
MitoTracker	Mitochondrion	25nM for 30 minutes	579nm	599nm	561nm Solid State
LysoTracker	Food Vacuole	50nM for 30 minutes	577nm	590nm	561nm Solid State
Draq5™	Nucleus	1□M	647nm	670nm	633nm HeNe
DB75	????	100nM-1□M	365nm	465nm	364nm UV

Table 3.2: Developmentally expressed genes in *P. falciparum*

Gene (PlasmoDB ID)	*Maximum Expression (hr)	Stage Expressed	Forward Primer (5'-3')	Reverse Primer (5'-3')
Trophozoite Antigen r45-like protein (PFD1175w)	16	Ring	ACGAGCTGACCCACCAAA	CATTTAAGTCTGTCTTCATTCTACTTCT
L-lactate dehydrogenase (PF13_0141)	21	Late Ring/ Early Trophozoite	ACGATTTGGCTGGAGCAGAT	TCTCTATTCCATTCTTTGTCACTCTTC
Isocitrate dehydrogenase (PF13_0242)	29	Trophozoite	CCAGACGGTGTTACGTGTGT	TTTTCTCCCTTTTGATAAGCTCTA
DNA primase (PFI0530c)	30	Trophozoite	AGATTGTCTCCTCAAAACCTTTATAG	GTTGTCTTCCCCAATGTTTTAA
Merozoite surface protein 7 (PF13_0197)	37	Schizont	CAAAGTGAAACAGATACTCAATCTAAAA	TGAAATGTCGATTCTCCTCCTT
Merozoite surface protein 1 (PFI1475w)	42	Schizont	AGCAAGCGAAACAACTGAAGA	TTGTTACCGTTGTTGTGTGTCCTA
Ribosomal protein S18 (PF11_0272)		Constitutive	GGCAACTGTTATATGTAAACAAGCA	GGGTAGGAGTACTCATAATATGTAGA

*Time post-invasion for maximum transcript levels detected by microarray (20)

Figure 3.1: DB75 inhibition of *P. falciparum*. The percent inhibition of parasite growth was measured with tritiated hypoxanthine for asynchronous parasites exposed to drug for 42 hours (grey line, open circle); synchronized ring-stage parasites exposed to drug for 36 hours (black line, closed square); synchronized rings-stage parasites exposed to drug for 96 hours (black line, open square); and synchronized trophozoite-stage parasites exposed to drug for 36 hours (black line, closed triangle).

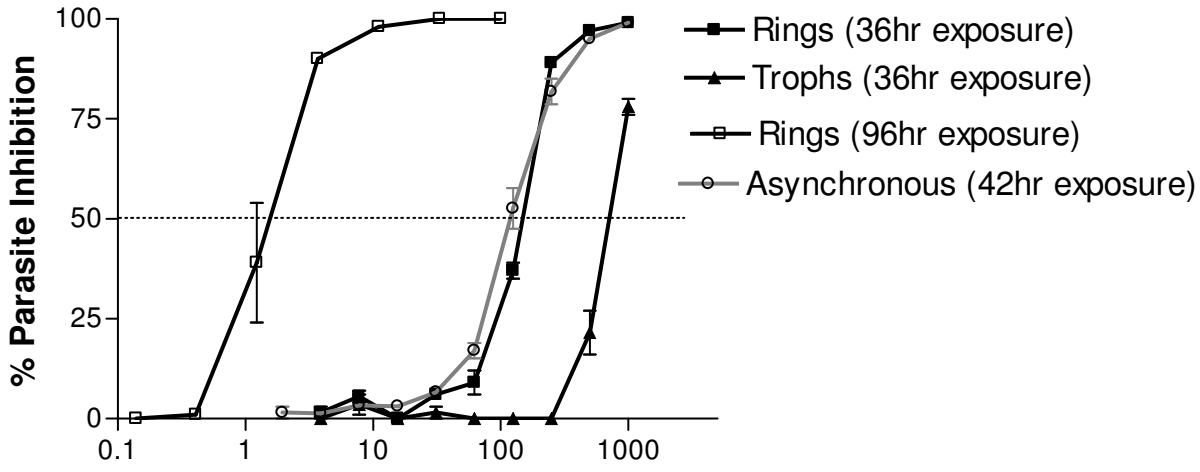

Figure 3.2: DB75 subcellular distribution in different *P. falciparum* life stages upon immediate cell entry (<4 hours). (A) 1μM DB75 (blue) and LysoTracker Red show no co-localization of the food vacuole of a trophozoite. (B) In a schizont, 1μM DB75 co-localizes with green nuclear Draq5™ stain but not MitoTracker Red. (C) 1μM DB75 fluorescence is not present in ring stage parasites. All images are representative.

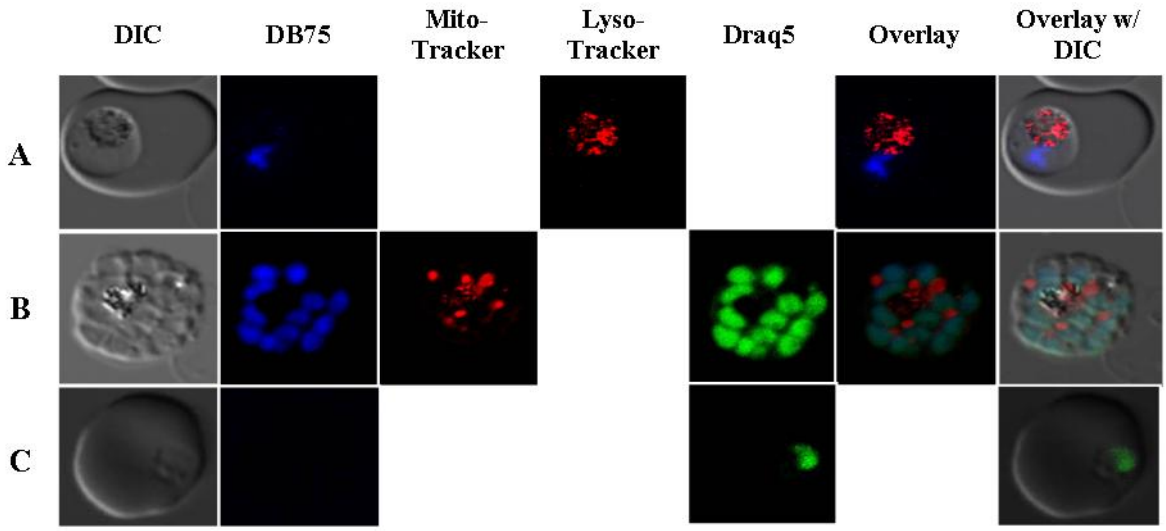

Figure 3.3: DB75 subcellular distribution following long term drug exposure. (A) Infected erythrocytes exposed to 100nM DB75 for 24 hours. Note co-localization of DB75 and nuclear DNA stain, Draq5™. (B) Drug was removed by washing at 24 hours and infected erythrocytes incubated for an additional 48 hours in drug-free medium. Note persistent co-localization of DB75 and Draq5™ in nucleus of pycnotic infected erythrocyte.

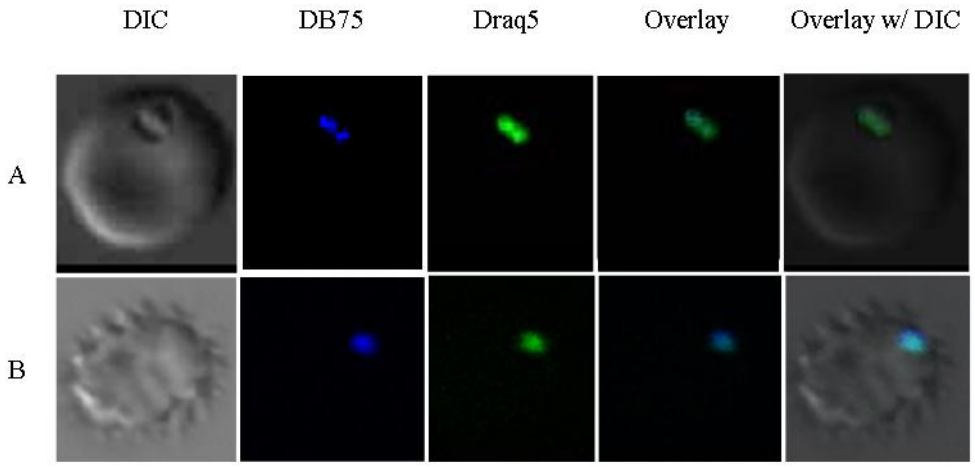

Figure 3.4: DB75 distribution in an erythrocyte infected with multiple parasites following 72 hours of exposure. DB75 emits at both 465nm (b) and 558nm (c) with extended exposure. The fluorescence emitted at these wavelengths overlay with Draq5™ (f and g).

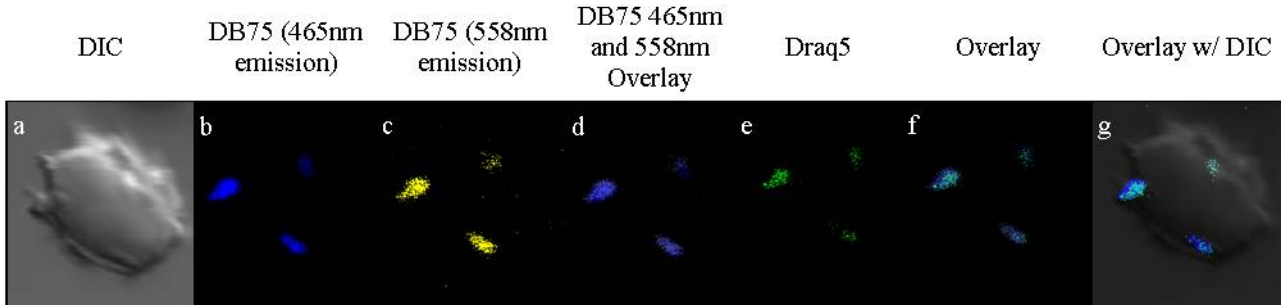

Figure 3.5: Parasite morphology with 96 hour continuous DB75 exposure. (a and b) Synchronized rings or (c and d) trophozoites (a and c) without treatment or (b and d) with exposure to 100nM DB75 (b and d) for 96 hours. The number of ring (yellow), trophozoite (green) and schizonts (purple) are shown per 1000 red blood cell over time. Note: the x-axis of (b) is on a different scale.

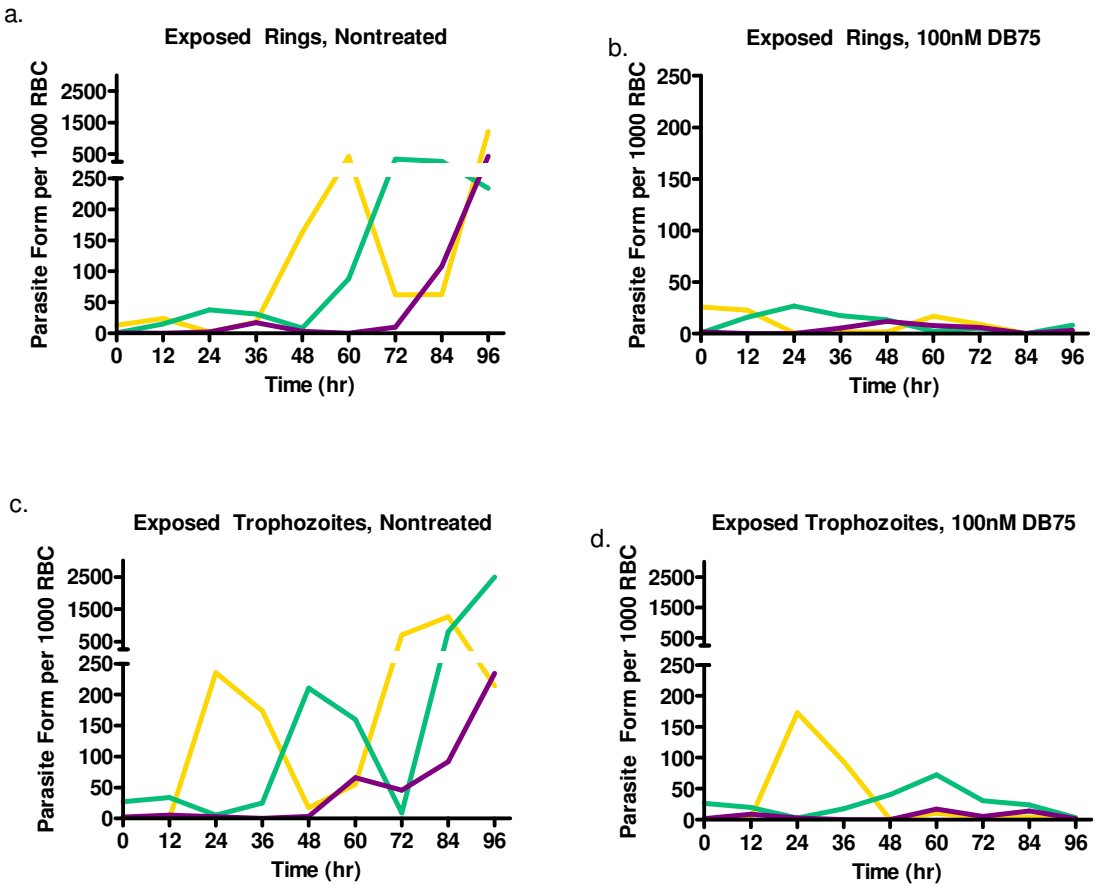

Figure 3.6: Parasite growth with 96 hour drug exposure. (a) Synchronized rings or (b) trophozoites were exposed to various concentrations of DB75 for 96 hours. Parasitemia was determined at 12 hour intervals for each DB75 drug concentration.

a.

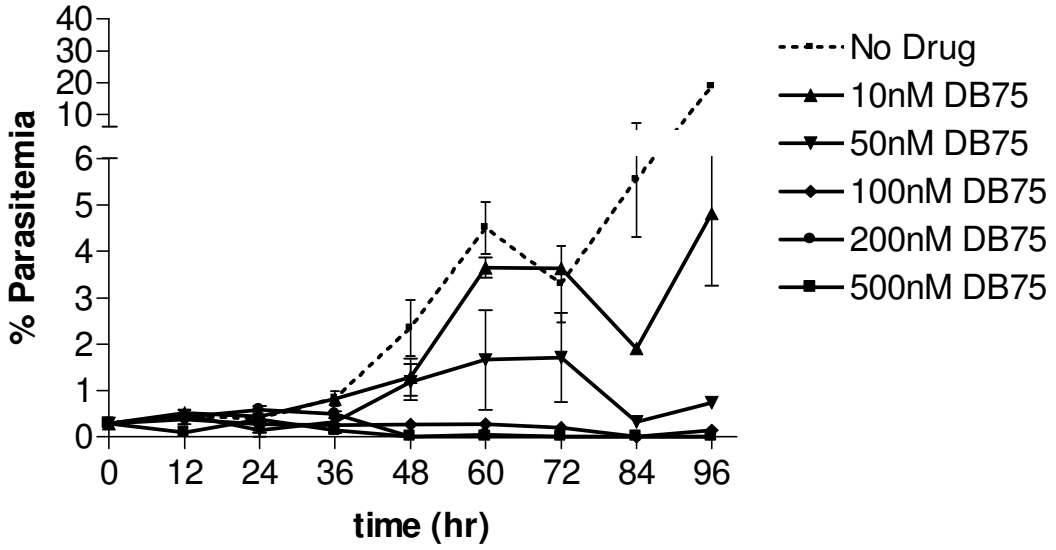

b.

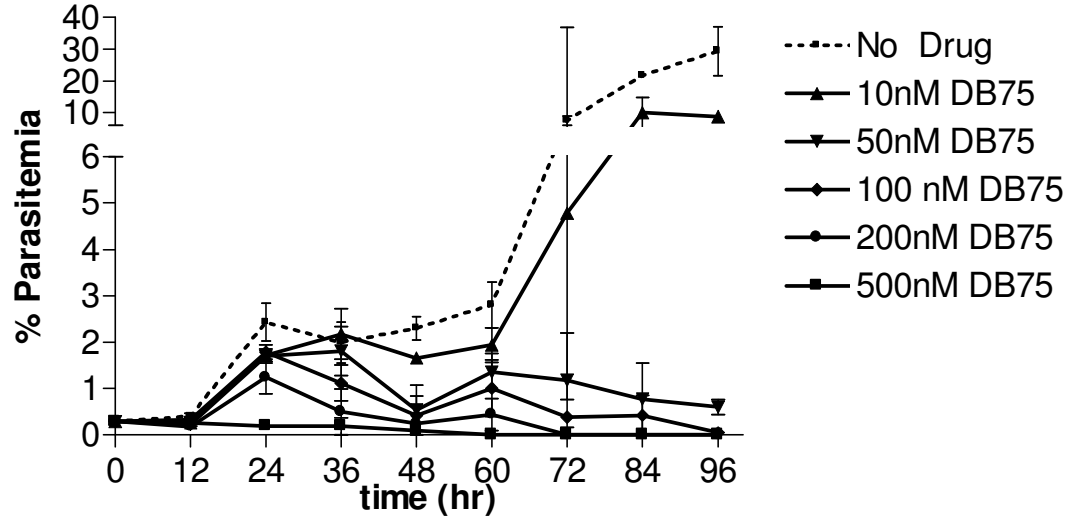

Figure 3.7: Parasitemia over time when DB75 drug pressure is removed after 48 hours of continuous exposure. (a) Synchronized rings or (b) trophozoites were exposed to various concentrations of DB75 for 48 hours before cells were washed and incubated an additional 48 hours without drug pressure.

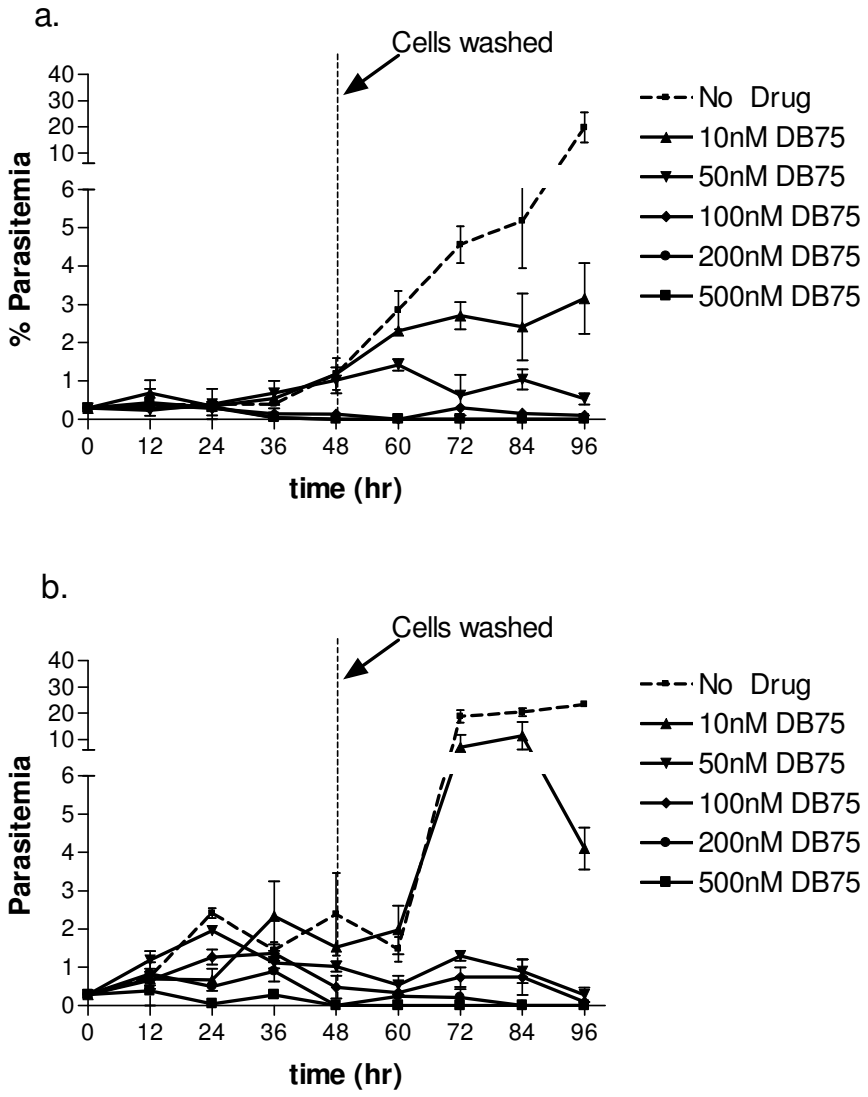

Figure 3.8 Effect of DB75 on peak expression time and intensity. Expression profiles for six developmentally expressed genes were compared in synchronized rings with exposure to 100nM (grey) or 500nM (black) DB75 or left untreated (white). (a) Time of invasion was approximated based on assessment of morphology, and peak expression post-invasion was estimated for all genes. (b) Expression intensity at time of peak expression was measured as the fold change in expression relative to the constitutively expressed 18s rRNA for exposed rings. Genes evaluated include: *trophozoite antigen r45-like* (Troph Ag); *lactate dehydrogenase* (ldh*), isocitrate dehydrogenase* (Iso); *DNA primase* (DNAp), *Merozoite surface protein-1* (MSP-1); *Merozoite surface protein-7*(MSP-7).

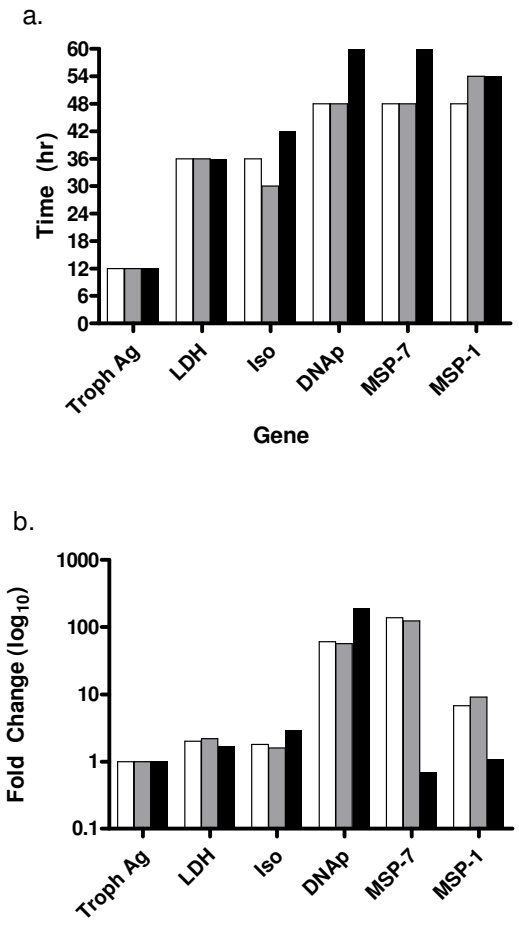

CHAPTER 4

DB75 interaction with other antimalarial compounds

PREFACE

The following chapter is in preparation for publication as a 1400-word "Notes" submission to Antimicrobial Agents and Chemotherapy. This chapter is an expanded version of the article prepared for publication. Contributing authors include: Anne Purfield, Richard R. Tidwell and Steven R. Meshnick. Anne Purfield is the primary author and has conducted all experiments and analyses. Stephanie Wallace assisted with parasite maintenance, and Jesse Kwiek contributed to the experimental design.

This research was supported by Medicines for Malaria Venture and the Bill and Melinda Gates Foundation.

CHAPTER 4

DB75 interaction with other antimalarial compounds

Introduction

DB289, [2,5-bis-(4-amidinophenyl)furan bis-*O*-methylamidoxime], is a promising new orally active antimicrobial compound (178). DB289 is the pro-drug of the active metabolite DB75, [2,5-bis-(4-amidinophenyl)furan], (175) which is effective against *P. falciparum*, *Pneumocystis jiroveci, Trypanosoma brucei,* and *Leishmania spp.* in vitro and in animal models (22, 153).

DB289 has shown promising activity against both malaria and African trypanosomiasis infections in humans. In a clinical study conducted in Thailand, DB289 (100 mg/day x 5 days) cured 22 of 23 (96%) *P. falciparum*-infected patients (178). The drug was well tolerated in patients and exhibited a mean ±SD parasite clearance time of 43h ±41 (178) which is comparable to the highly efficacious combination of atovaquone and proguanil (41.9±22.1) (82).

Because *P. falciparum* can develop resistance to monotherapy quickly, the WHO recommends that all new treatment regimens be combinations of antimalarials (1). For partner drugs to be effective in practice, they should ideally be synergistic and certainly not be antagonistic. DB289 represents a safe, effective and structurally novel compound that may be used in combination for treatment of *P. falciparum* malaria (178).

The aim of this study was to characterize the interactions of the active metabolite, DB75, with other antimalarials in order to help identify the best partner drug for combination therapy. We report here that in vitro activity of DB75 was indifferent when combined with

10 antimalarial compounds that include: atovaquone, artemisinin, amodiaquine, azithromycin, chloroquine, tafenoquine, pyronaridine, piperaquine, tetracycline and mefloquine. DB75 and clindamycin appeared to act in a synergistic manner with drug exposures of 42 or 66 hours. However, when cells were exposed to these drugs for 96 hours, the combination had an indifferent effect on parasite inhibition.

Materials and Methods

Parasite Culture

3D7 "wild type", drug susceptible *P. falciparum* was maintained in O+ human erythrocytes (Research Blood Concepts, Brighton, MA) supplemented with 1640 RPMI with 25mM HEPES (Sigma Aldrich, St. Louis, MO), 2mM L-glutamine (Gibco, Carlsbad, CA), 0.45% (w/v) glucose (Sigma Aldrich, St. Louis, MO), 0.05ng/ml gentamycin (Sigma Aldrich, St. Louis, MO), 0.1 mM hypoxanthine and 10% O+ human serum (Research Blood Concepts, Brighton, MA). Cultures were maintained at 37 ^{o}C by a modified version of the Trager and Jensen method in candle jars with low oxygen tension (155).

42 hour [^{3}H]-Hypoxanthine Incorporation Assay

To measure in vitro drug sensitivity, we used [^{3}H]-hypoxanthine incorporated into parasite-synthesized DNA (41). Parasite cultures were diluted to 0.7% parasitemia in 2% (v/v) erythrocytes and complete medium without supplemental hypoxanthine. 180µl of infected red blood cells were sub-cultured in 96-well flat bottom microtitre plates with 10µL of DB75. DB75 was tested in combination with: amodiaquine, artemisinin, atovaquone, azithromycin, chloroquine, clindamycin, mefloquine, piperaquine, pyronaridine, tafenoquine and tetracycline. Atovaquone and proguanil were tested in combination as a positive control to validate the method. All compounds were dissolved in water, 95% ethanol or DMSO for

stock solutions. Serial dilutions were made from the stock solution in medium without supplemental hypoxanthine. 10µl of diluted drug was added to infected red blood cells with DB75 in 96-well plates.

To test the sensitivity of parasites to variable concentrations of two drugs in combination, we used a checkerboard matrix of decreasing DB75 concentrations across the plate with concentrations of the partner drug decreasing down the plate (41). The drug concentration ranged from 5-10X above and below the IC50 (concentration for 50% of maximal growth inhibition) of the drug. In addition, we tested each drug alone to control for the sensitivity in the absence of a partner drug in combination. We also controlled for: 1) parasite growth in the absence of drug (maximum growth) and 2) erythrocyte uptake of [^{3}H]-hypoxanthine (background).

To measure growth in 42 hours, the 96-well plates were incubated for 24 hours prior to the addition of 0.5µCi of [^{3}H]-hypoxanthine diluted in hypoxanthine-free medium (25µl/well). The cells were incubated for an additional 18 hours and harvested using an Inotech cell harvester and glass fiber filter paper (Inotech Systems International, INC.). Radioactivity of samples was determined in a liquid scintillation counter (Beckman-Coulter). For each drug combination, the assay was repeated two or three times.

66 hour [^{3}H]-Hypoxanthine Incorporation Assay

To measure growth in 66 hours, the same methods were followed as described above except a 0.4% parasitemia was used and [^{3}H]-hypoxanthine was added to the 96-well plates following 48 hours of incubation. The parasites were incubated for an additional 18 hours and harvested as described above. DB75 was tested in combination with tetracycline, clindamycin, azithromycin, and tafenoquine at 66 hours for growth inhibition.

96 hour [^{3}H]-Hypoxanthine Incorporation Assay

To measure growth in 96 hours with clindamycin, we used 0.3% sorbitol-synchronized ring cultures (84). The [^{3}H]-hypoxanthine was added to the 96-well plates following a 48 hour incubation. Cells were incubated an additional 48 hours prior to harvesting and scintillation counting. DB75 was tested in combination with clindamycin at 96 hours.

Interpretation of Results

To determine the IC50 value from percent inhibition (Equation 1), we used the sigmoidal dose response equation (Equation 2) from the nonlinear regression analysis of Graphpad Prism® (version 3.0). The maximum growth was calculated from the average count per minute (cpm) of 10 control wells with infected erythrocytes but no drug. The background is defined as the average cpm from 10 wells with uninfected erythrocytes.

$$\text{Equation 1: Percent Inhibition} = \frac{CPM_i - \text{Background}}{\text{Max. Growth} - \text{Background}} * 100$$

$$\text{Equation 2: } Y = \frac{\text{Bottom} + (\text{Top}-\text{Bottom})}{(1+10^{(\text{LogEC50}-X)}*\text{HillSlope})}$$

Where X is the logarithm of drug concentration; Y is the percent inhibition; “Bottom” is minimum percent inhibition (0); and “Top” is maximum percent inhibition (100).

We evaluated the effect using isobolograms, fractional inhibitory concentrations (FIC) (Equation 3) and sum FIC values to determine the relationship between DB75 and the partner drug (10, 15) .

Equation 3: $FIC = \frac{\text{IC50 of DB75 in combination}}{\text{IC50 of DB75 alone}} + \frac{\text{IC50 of partner drug in combination}}{\text{IC50 of partner drug alone}}$

For an isobologram, the IC50 values of DB75 with the partner drug at each combination of concentration were plotted against the IC50 values of the partner drug in combination with DB75 dilutions. A line was drawn to connect the IC50 values of each drug. If the points on the graph fell under the line, the interaction was determined to be synergistic. If the points fell along the line, the interaction was indifferent and if the points fell above the line the interaction was antagonistic.

The FIC was used to normalize against a concentration-dependent bias. FIC values were plotted as isobolograms using FIC values instead of IC50 values (Figure 4.1) (25). A line was drawn between 1.0 on the x and 1.0 on the y axis. The relationship was evaluated by the location of the FIC values below, above or on the line, as described above (25).

The mean sum FIC value was used to quantify the drugs' effect in combination. For the sum FIC of each partner drug combination, the FIC values were added together. A value above 2.0 indicated antagonism while values less than 0.5 suggest synergism. Sum FIC's that fell between 0.5 and 2.0 were indicative of an indifferent relationship (10, 15, 25).

Results

To find a potential partner for DB75, the compound was tested in combination with 11 current and investigational antimalarials. As a positive control, atovaquone and proguanil showed synergy in combination (sum FIC=0.63) (Figure 4.1a). The antimalarials tested in combination represented six classes of compounds, including aryl amino alcohols, 4-

aminoquinolines, 8-aminoquinolines, antimicrobials, peroxides and naphthoquinones; and all results are summarized in Table 4.1.

The structurally similar aryl amino alcohols, 4-aminoquinoline and 8-aminoquinoline compounds all produced an indifferent effect in combination with DB75. The 4-aminoquinoline compounds tested, including chloroquine, amodiaquine, pyronaridine and piperaquine; produced some of the highest sum FIC values of all compounds tested although well below values considered antagonistic (mean±SD sum FIC=1.21±0.09). Chloroquine, in particular, had the highest mean±SD sum FIC at 1.31±.12 (Figure 4.1h). The only 8-aminoquinoline compound tested was tafenoquine, which was indifferent in combination with DB75 at 42 hours (mean±SD sum FIC=1.00±0.06) (Figure 4.1d). Tafenoquine was also tested in combination for 66 hours because it is a long acting drug, but it was still indifferent with DB75 (mean±SD sum FIC=1.05±0.06) (Figure 4.2b). Mefloquine, an aryl amino alcohol, was indifferent in combination with DB75 when tested for 42 hours (mean±SD sum FIC=1.08±.14) (Figure 4.1i).

The peroxides and naphthoquinones are structurally-unique antimalarials. In combination with DB75, compounds from both classes had an indifferent effect on parasite growth (Figure 4.2g and k). The fast-acting peroxide, artemisinin, had a mean±SD sum FIC of 1.19±0.15. Atovaquone, a naphthoquinone, was also indifferent in combination with DB75 (mean±SD sum FIC=0.94±0.14).

The long-acting antibiotic compounds, azithromycin, clindamycin and tetracycline were also tested in combination with DB75 for short and extended exposures. First, both azithromycin and tetracycline were indifferent when tested for 42-hour (Table 4.1 and Figure

4.1b and f) or 66-hour exposures (Table 4.1 and Figure 4.2a and c). However, results for the clindamycin-DB75 combination were less clear-cut.

As previously described, clindamycin alone exhibited a biphasic concentration response (137). Complete inhibition was not achieved with clindamycin alone at 42- or 66-hour exposures even with hemolytic concentrations of more than 100μM (Figure 4.3a and b). For this reason, the interaction with DB75 could not be assessed by the traditional FIC or sum FIC methods. However, it was clear from the concentration response curves that clindamycin has an effect on the DB75 IC50 at 42 and 66 hours (Figure 4.3a and d). Clindamycin concentrations as low as 164nM enhanced the inhibitory effect of DB75 alone by nearly tenfold (Figure 4.3a and d). Alone, DB75 exhibited an IC50 of 82nM but in combination with 164nM clindamycin, the IC50 of DB75 was reduced to 8.9nM. When clindamycin and DB75 were incubated together for 66 hours, DB75 concentration response curves suggest clindamycin reduced the DB75 IC50 albeit less impressive than the effect seen in the 42-hour assay (Figure 4.3b). For example, the IC50 of DB75 is reduced from 95nM when used alone to 14nM when used in combination with 123nM clindamycin (Figure 4.3b)

Since both clindamycin and DB75 have long onsets of action in vivo (59, 178), we determined whether the "enhancing" effect was apparent with an extended incubation period equal to two complete life cycles (96 hours). By itself, DB75 is much more potent after long incubations than after short incubations (Table 4.2). However, when DB75 and clindamycin were incubated in combination for 96 hours, a sigmoidal dose response was evident for clindamycin alone. This allowed us to calculate an IC50 value to use with standard FIC methods for analysis. At 96 hours the interaction was indifferent with a mean±SD sum FIC

of 1.10±0.16 (Figure 4.2d). This suggests that the combination of drugs may not be synergistic in the classical sense, but that the combination may accelerate parasite killing upfront.

Discussion

DB75 manifested indifferent relationships with 10 of the drugs tested in the 42-hour assay. Three of these drugs (tetracycline, tafenoquine and piperaquine) also showed indifference even with extended incubations. However, clindamycin reduced the DB75 IC50 with 42 and 66-hour assays, although the effect was indifferent when DB75 and clindamycin were tested in combination for 96 hours.

The indifferent effect that DB75 had with drugs in combination may suggest an independent mechanism. DB75 is known to bind the minor groove of DNA and may inhibit DNA replication or gene transcription (98). Combination therapy using drugs with unique mechanisms was proposed to slow the development of resistance to each partner drug (169). Taken together, an independent mechanism and indifferent drug interactions suggest that DB75 could be successfully partnered with a variety of antimalarials including: amodiaquine, artemisinin, atovaquone, azithromycin, chloroquine, clindamycin, mefloquine, piperaquine, pyronaridine, tafenoquine and tetracycline. However, the pharmacokinetic profiles of each drug in combination should be similar to prevent resistance from developing to partner drugs with longer elimination (169). The elimination half-life of DB75 is 53 hours (Richard R. Tidwell, personal communication). Of the 11 compounds tested in combination with DB75, two have similar elimination half-lifes: atovaquone (50-84hr) and azithromycin (59-72hr) (30, 69).

Our results suggest that clindamycin enhances parasite killing in combination with DB75 for 42 or 66 hours, but not at 96 hours. The synergy observed with shorter incubations suggests DB75 has a mechanism of action unique from clindamycin, although both drugs have long onsets of action (24, 178). Clindamycin is believed to target protein synthesis in the apicoplast of the parasite (36, 53, 123). The apicoplast is unique to the apicomplexan parasites, contains an independent genome (35-kb) and is critical for parasite survival (reviewed in (134)). DB75, on the other hand, possibly targets nuclear activity in *P. falciparum*, as proposed in Chapter 3 of this thesis.

The indifferent effect of DB75 and clindamycin at 96 hours may be a consequence of the drugs' long onsets of action. Both drugs exhibit delayed death phenotypes, in which the antimalarial effect occurs in the progeny of parasites exposed to drug (Chapter 3 of this dissertation and (24, 36). For clindamycin, the progeny are unable to replicate apicoplasts, which leads to arrested development at the schizont stage and incomplete schizogeny (rupture of host cells and invasion of uninfected red blood cells) (36). We proposed in Chapter 3 of this dissertation that the antimalarial effect of DB75 is stage-specific. Ring-stage parasites must be exposed to DB75, and then parasite development is delayed and arrested at the trophozoite stage. When trophozoites are exposed to DB75, the same antimalarial effect is observed in the progeny of exposed cells. However, both DB75 and clindamycin inhibit the emergence of a second- or third- generation ring population, depending on the drug and the development stage at time of initial exposure. Based on the independent mechanisms of DB75 and clindamycin, it possible that synergy occurs between the drugs in the first two life cycles because the drugs have unique targets and life stages, but by the end of the 2nd complete life cycle both drugs have effectively eliminated parasites.

Despite the synergy observed, a slow onset of action and short half life of clindamycin would not be ideal when paired with DB75, which has a long half life and long onset of action, for treatment of malaria in endemic areas. However, this combination may provide effective chemoprophylaxis for malaria because neither drug has been used for malaria treatment to date. Therefore, it is likely that there is no resistance to either of these drugs, and when used in combination for prophylaxis, resistance would be slow to emerge. Further studies need to be conducted to determine the effect of clindamycin and DB75 on parasite morphology and growth over two complete life cycles to determine if the drugs in combination result in parasite death earlier in the life cycle than each drug alone. Also, this combination should be tested in vivo for the therapeutic effect to treat or prevent malaria infection.

This study has few limitations. First, only one parasite strain, 3D7, was used to test for the inhibitory effect of DB75 in combination with other antimalarials. 3D7 is considered a "wild type", drug sensitive strain of *P. falciparum*. Other strains that exhibit decreased susceptibility to various drugs may reflect parasite populations in malaria endemic areas. Second, clindamycin exhibits a biphasic killing curve in 42- and 66-hour assays. It is difficult to determine the IC50 from biphasic curves, therefore the synergy of DB75 and clindamycin at these time points was determined from the effect of clindamycin on the DB75 IC50 instead of the usual method based on FIC.

In summary, we have demonstrated the effect of DB75 in combination with 11 antimalarial drugs. All drugs tested with DB75 exhibited an indifferent effect on parasite growth except clindamycin. Clindamycin promoted DB75 action at 42 and 66 hours but the

interaction was indifferent at 96 hours. This study suggests that DB75 has an independent mechanism from the drugs tested, and all may be used in combination with DB75.

Figure 4.1: DB75-partner drug interactions with 42-hour co-incubation at various concentration ratios. (b-k) Growth was measured using [^{3}H]-hypoxanthine growth assays for all drugs tested in combination with DB75. (a) Atovaquone and proguanil were used in combination to show true synergy. (a) A concave isobologram indicates synergy; a convex one indicates antagonism (none shown) and (b-k) points along the straight line indicate indifference.

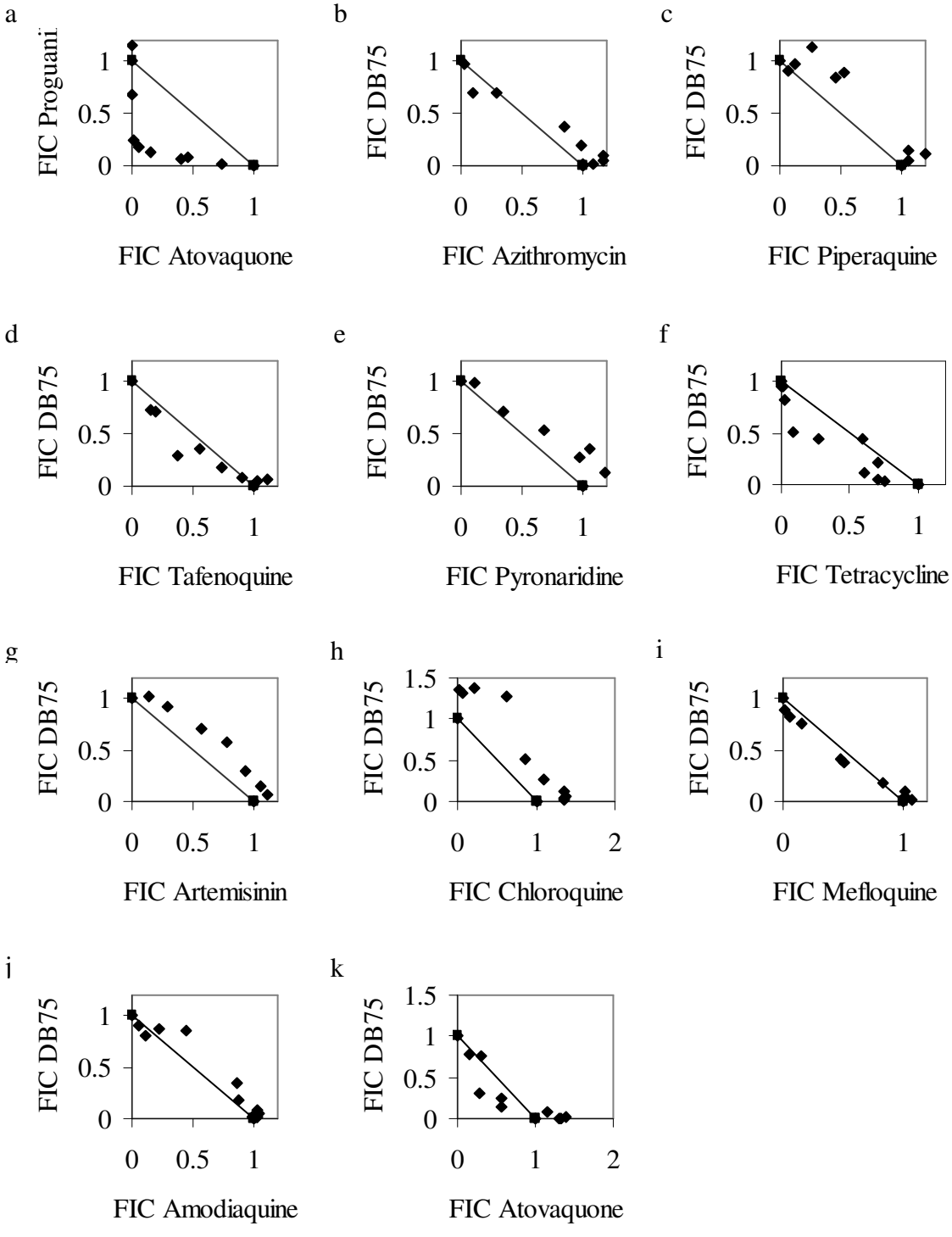

Figure 4.2: DB75-partner drug interaction with (a-c) 66-hour or 96-hour (d) co-incubation. All interactions shown are indifferent.

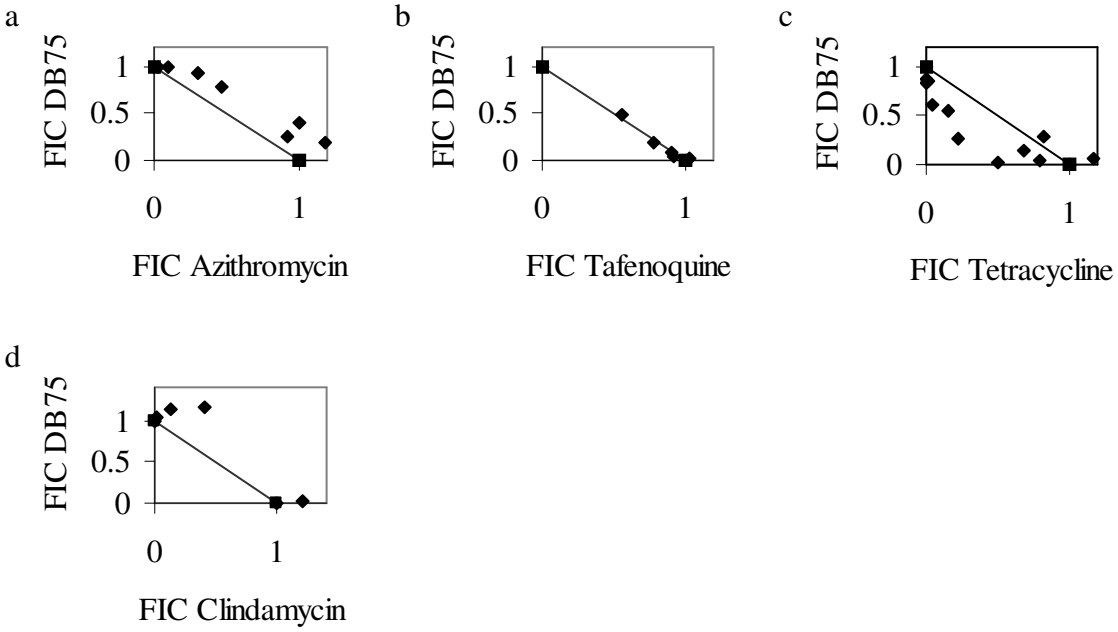

Figure 4.3: Clindamycin effect on DB75 IC50. Parasite inhibition was measured with DB75 and clindamycin co-incubated for (a) 42-hour, (b) 66-hour and (c) 96-hour. 3-fold serial dilutions of clindamycin (closed square) were used with a DB75 only control. Concentrations of clindamycin are shown to the right of each dose-response curve. (d) Low concentrations of clindamycin enhance the effect of DB75 by reducing the IC50.

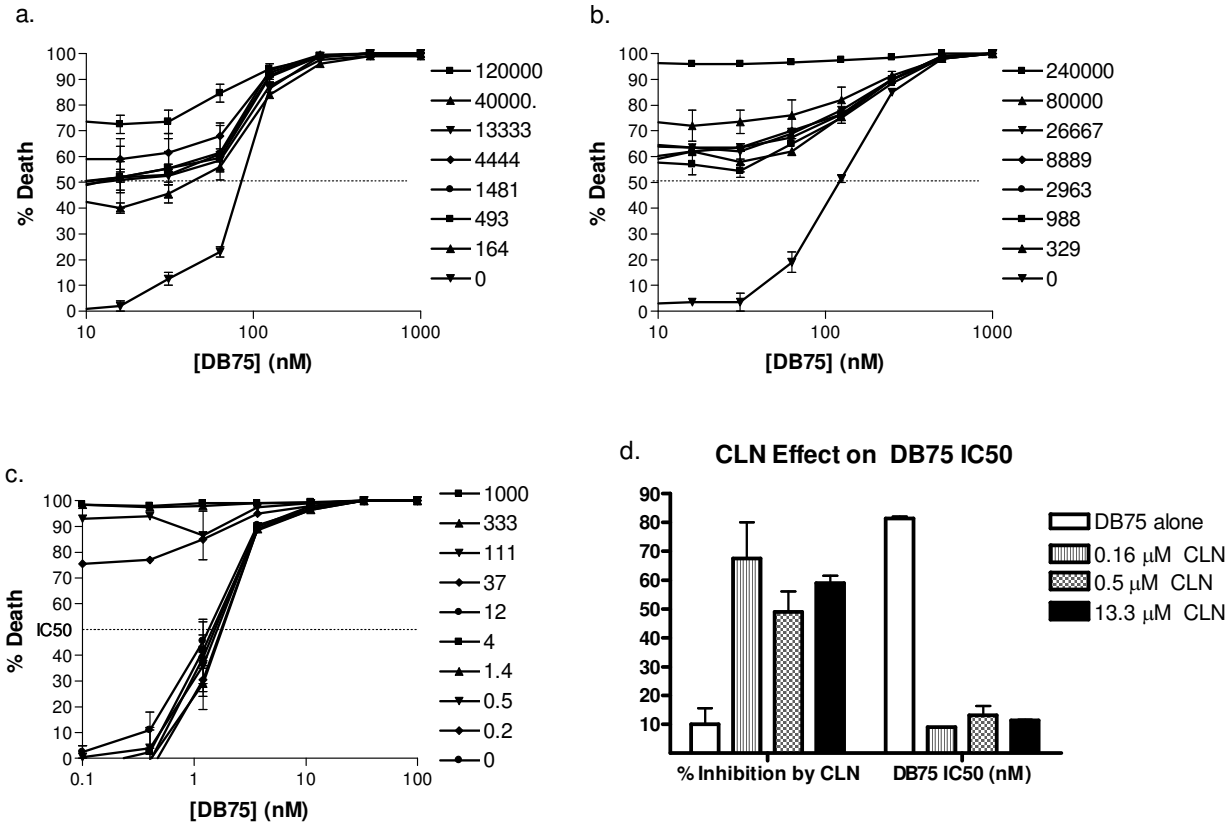

Table 4.1: Results for antimalarial agents in combination with DB75[a]

	42 hour Assay		66 hour Assay		96 hour Assay	
Partner Drug	**FIC**	**Sum FIC (±SD)**	**FIC**	**Sum FIC (±SD)**	**FIC**	**Sum FIC (±SD)**
Clindamycin	S	N/A	S	N/A	I	1.18[b]
Tetracycline	I	0.88 (0.08)	I	1.04 (0.19)		
Atovaquone	I	0.94 (0.14)				
Tafenoquine	I	1.00 (0.06)	I	1.05 (0.06)		
Mefloquine	I	1.08 (0.14)				
Amodiaquine	I	1.09 (0.03)				
Artemisinin	I	1.19 (0.15)				
Piperaquine	I	1.23 (0.04)				
Azithromycin	I	1.20 (0.18)	I	1.29 (0.13)		
Pyronaridine	I	1.20 (0.02)				
Chloroquine	I	1.31 (0.12)				
Atovaquone and Proguanil	I	0.63				

[a] values are reported as means and standard deviation of 2-3 assays

[b] Synchronized rings were used for the 96 hour assay

S= synergistic, I-indifferent

Table 4.2: DB75 IC50 decreases with extended exposure

Exposure (hr)	DB75 IC50 (nM)
42	128 ± 51
66	139 ± 43
96	3.7 ± 0.76

CHAPTER V
Summary and Future Directions

CHAPTER V

Summary and Future Directions

This dissertation focuses on the mechanism of resistance and mode of action for drugs against *P. falciparum*. With widespread existence of drug resistant parasites, there is an increasing need for evaluation of resistance mechanisms and new drugs to combat malaria. In this report, we provide a new method for monitoring drug resistance. Also, we attempt to elucidate the mechanism of action for DB75, the prodrug of the antimalarial compound DB289. Finally, we determine the antimalarial effect of DB75 in combination with other antimalarial drugs in vitro.

We report a new method for *pfmdr1* SNP analysis allows for rapid identification of mutations associated with drug resistance. Real time PCR is sensitive and specific method that may be used for high-throughput analysis of parasite genotypes. Alternative methods require parasites to be sub-cultured for drug-susceptibility testing and analysis of genotype using PCR and sequencing or restriction fragment length polymorphism (RFLP). Real time PCR is less labor extensive and incurs less cost per reaction than these methods. Future epidemiological studies may use this method as a public health tool to survey parasite populations for drug resistance and to predict treatment failure in individuals. Ultimately, this tool may provide insight about the temporal evolution and geographical spread of parasite populations exhibiting drug resistance. With adequate surveillance data, healthcare officials may evaluate and, if necessary, adjust policy regarding antimalarial treatment. Proper action may thwart the spread of antimalarial drug resistance, prolong the use of treatments and ultimately, reduce mortality.

There is an urgent need for new antimalarial compounds with the rapid emergence and spread of resistance to currently used drugs. We report antimalarial characteristics for the metabolite, DB75, of the novel antimicrobial drug, DB289. DB289 is currently in development for treatment of falciparum malaria, however the mode of action against falciparum parasites is unknown. We propose a partial mechanism of DB75.

DB75 targets the nucleus of the parasite. Our results from ultraviolet confocal microscopy show DB75 localization exclusively in the nucleus of parasites in culture. Previous reports have suggested the target may be the mitochondrion, acidocalcisome or food vacuole (97, 147). However, we show DB75 only accumulates in the nucleus with short or long term exposure. This is consistent with data showing DB75 binds to AT rich sequences of DNA (98). To date, no other antimalarial compound has been shown to target the nucleus, suggesting DB75 has a unique target in *P. falciparum*.

We also propose the mechanism of action for DB75 is stage specific. Assessment of parasite morphologies after DB75 exposure shows early stage parasites are more sensitive to drug than late stage parasites. Parasites must be exposed during the ring stage for effective inhibition. This may explain the need for a 5 day dosing regimen for effective parasite clearance in vivo. Our data suggests in vivo, early stage parasites are effectively cleared in the first 48 hours of treatment. However all parasites in the trophozoite or schizont stages must advance to the next life cycle and be exposed as rings before elimination.

The increased sensitivity of rings suggests the DB75 mode of action involves interruption of a stage-dependent process such as nucleotide synthesis. When cells are treated with aphidicolin to arrest DNA synthesis a similar effect is observed (70). Both aphidicolin and DB75 stall parasite maturation as well. Aphidicolin arrests development at the late

trophozoite-schizont stage (70). However, DB75 stalls maturation at the early-mid trophozoite stage, suggesting that an additional mechanism might be involved. Further studies are needed to evaluate the effect of DB75 on other nuclear activities such as enzyme activity and mRNA translation.

We report here that the DB75 mechanism is not likely to include inhibition of developmental gene transcription. The expression profiles of six developmentally expressed *P. falciparum* genes were not significantly altered with therapeutic concentrations of DB75 (100nM). However, a higher concentration of DB75 (500nM) altered the profiles of some genes in a manner consistent with delayed maturation. We conclude that these changes observed in select genes are not responsible for the delay in maturation because they occur concurrently with the stalled cell cycle. However, further studies are necessary using microarray analysis to determine the effect of DB75 on developmental regulation of all genes.

We observed a sharp increase of *DNA primase* expression with 500nM DB75. Although a similar result was obtained with atovaquone treated cells, more extensive studies with atovaquone and other antimalarial drugs may determine the whether this results is drug-specific or significant to the mechanism of DB75.

Taken together, our data suggests DB75 has a unique target in *P. falciparum*. Our results are consistent with a mechanism that includes inhibition of DNA synthesis with other nuclear activity possible.

With a unique target in, DB75 is an ideal candidate combination therapy. We show that DB75 is indifferent in combination with atovaquone, azithromycin, piperaquine, tafenoquine, pyronaridine, tetracycline, artemisinin, chloroquine, mefloquine amodiaquine and

atovaquone. This is further support that DB75 has an independent target and/or mechanism from currently used antimalarials. Further, our results suggest that some synergism may exist when DB75 is used in combination with clindamycin and additional studies need to be carried out to identify the extent of this interaction. If these two drugs produce effective synergism, the combination may be a useful tool to combat malaria in resource poor regions because clindamycin is an inexpensive drug.

Taken together, this work contributes to the arsenal of tools for surveillance of falciparum malaria drug resistance and partially elucidates a mechanism of action for a novel antimalarial diamidine that may be used for malaria therapy.

REFERENCES

1. 2001. Antimalarial Drug Combination Therapy, p. 36. *In* M. Geyer (ed.), WHO Technical Consultation. World Health Organization, Geneva, Switzerland.

2. 2006. Schema of the Lifecycle of Malaria. *In* D. o. P. D. National Center for Infectious Diseases (ed.), vol. 2007. Centers for Disease Control and Prevention, Malaria.

3. **Afonina, I., M. Zivarts, I. Kutyavin, E. Lukhtanov, H. Gamper, and R. B. Meyer.** 1997. Efficient priming of PCR with short oligonucleotides conjugated to a minor groove binder. Nucleic Acids Res **25:**2657-60.

4. **Alker, A. P., P. Lim, R. Sem, N. K. Shah, P. Yi, D. M. Bouth, R. Tsuyuoka, J. D. Maguire, T. Fandeur, F. Ariey, C. Wongsrichanalai, and S. R. Meshnick.** 2007. Pfmdr1 and in vivo resistance to artesunate-mefloquine in falciparum malaria on the Cambodian-Thai border. Am J Trop Med Hyg **76:**641-7.

5. **Antoniou, T., and K. A. Gough.** 2005. Early-onset pentamidine-associated second-degree heart block and sinus bradycardia: case report and review of the literature. Pharmacotherapy **25:**899-903.

6. **Armstrong, D., and J. Cohen.** 1999. Infectious diseases. Mosby, London ; Philadelphia.

7. **Athri, P., T. Wenzler, P. Ruiz, R. Brun, D. W. Boykin, R. Tidwell, and W. D. Wilson.** 2006. 3D QSAR on a library of heterocyclic diamidine derivatives with antiparasitic activity. Bioorg Med Chem **14:**3144-52.

8. **Basselin, M., M. A. Badet-Denisot, and M. Robert-Gero.** 1998. Modification of kinetoplast DNA minicircle composition in pentamidine-resistant Leishmania. Acta Trop **70:**43-61.

9. **Bathurst, I., and C. Hentschel.** 2006. Medicines for Malaria Venture: sustaining antimalarial drug development. Trends Parasitol **22:**301-7.

10. **Bell, A.** 2005. Antimalarial drug synergism and antagonism: mechanistic and clinical significance. FEMS Microbiol Lett **253:**171-84.

11. **Bell, C. A., M. Cory, T. A. Fairley, J. E. Hall, and R. R. Tidwell.** 1991. Structure-activity relationships of pentamidine analogs against Giardia lamblia and correlation of antigiardial activity with DNA-binding affinity. Antimicrob Agents Chemother **35:**1099-107.

12. **Bell, C. A., C. C. Dykstra, N. A. Naiman, M. Cory, T. A. Fairley, and R. R. Tidwell.** 1993. Structure-activity studies of dicationically substituted bis-benzimidazoles against Giardia lamblia: correlation of antigiardial activity with DNA binding affinity and giardial topoisomerase II inhibition. Antimicrob Agents Chemother **37:**2668-73.

13. **Bell, C. A., J. E. Hall, D. E. Kyle, M. Grogl, K. A. Ohemeng, M. A. Allen, and R. R. Tidwell.** 1990. Structure-activity relationships of analogs of pentamidine against Plasmodium falciparum and Leishmania mexicana amazonensis. Antimicrob Agents Chemother **34:**1381-6.

14. **Benaim, G., C. Lopez-Estrano, R. Docampo, and S. N. Moreno.** 1993. A calmodulin-stimulated Ca2+ pump in plasma-membrane vesicles from Trypanosoma brucei; selective inhibition by pentamidine. Biochem J **296 (Pt 3):**759-63.

15. **Berenbaum, M. C.** 1978. A method for testing for synergy with any number of agents. J Infect Dis **137:**122-30.

16. **Berens, N., B. Schwoebel, S. Jordan, V. Vanisaveth, R. Phetsouvanh, E. M. Christophel, S. Phompida, and T. Jelinek.** 2003. Plasmodium falciparum: correlation of in vivo resistance to chloroquine and antifolates with genetic polymorphisms in isolates from the south of Lao PDR. Trop Med Int Health **8:**775-82.

17. **Boyd, M. F., and S. F. Kitchen.** 1937. Observations on Induced Falciparum Malaria. Am J Trop Med **s1-17:**213-235.

18. **Boykin, D. W., A. Kumar, J. E. Hall, B. C. Bender, and R. R. Tidwell.** 1996. Anti-pneumocystis activity of bis-amidoximes and bis-o-alkylamidoximes prodrugs. Bioorganic & Medicinal Chemistry Letters **6:**3017-3020.

19. **Boykin, D. W., A. Kumar, J. Spychala, M. Zhou, R. J. Lombardy, W. D. Wilson, C. C. Dykstra, S. K. Jones, J. E. Hall, R. R. Tidwell, and et al.** 1995. Dicationic diarylfurans as anti-Pneumocystis carinii agents. J Med Chem **38:**912-6.

20. **Bozdech, Z., Llin, M. s, B. L. Pulliam, E. D. Wong, J. Zhu, and J. L. DeRisi.** 2003. The Transcriptome of the Intraerythrocytic Developmental Cycle of Plasmodium falciparum. PLoS Biology **1:**e5.

21. **Bray, P. G., M. P. Barrett, S. A. Ward, and H. P. de Koning.** 2003. Pentamidine uptake and resistance in pathogenic protozoa: past, present and future. Trends Parasitol **19:**232-9.

22. **Brendle, J. J., A. Outlaw, A. Kumar, D. W. Boykin, D. A. Patrick, R. R. Tidwell, and K. A. Werbovetz.** 2002. Antileishmanial activities of several classes of aromatic dications. Antimicrob Agents Chemother **46:**797-807.

23. **Brockman, A., R. N. Price, M. van Vugt, D. G. Heppner, D. Walsh, P. Sookto, T. Wimonwattrawatee, S. Looareesuwan, N. J. White, and F. Nosten.** 2000. Plasmodium falciparum antimalarial drug susceptibility on the north-western border of Thailand during five years of extensive use of artesunate-mefloquine. Trans R Soc Trop Med Hyg **94:**537-44.

24. **Burkhardt, D., J. Wiesner, N. Stoesser, M. Ramharter, A.-C. Uhlemann, S. Issifou, H. Jomaa, S. Krishna, P. G. Kremsner, and S. Borrmann.** 2007. Delayed parasite elimination in human infections treated with clindamycin parallels `delayed death' of Plasmodium falciparum in vitro. International Journal for Parasitology **37:**777-785.

25. **Canfield, C. J., M. Pudney, and W. E. Gutteridge.** 1995. Interactions of atovaquone with other antimalarial drugs against Plasmodium falciparum in vitro. Exp Parasitol **80:**373-81.

26. **Chavalitshewinkoon, P., E. de Vries, J. G. Stam, F. F. Franssen, P. C. van der Vliet, and J. P. Overdulve.** 1993. Purification and characterization of DNA polymerases from Plasmodium falciparum. Mol Biochem Parasitol **61:**243-53.

27. **Chou, A. C., R. Chevli, and C. D. Fitch.** 1980. Ferriprotoporphyrin IX fulfills the criteria for identification as the chloroquine receptor of malaria parasites. Biochemistry **19:**1543-9.

28. **Choubey, V., P. Maity, M. Guha, S. Kumar, K. Srivastava, S. K. Puri, and U. Bandyopadhyay.** 2007. Inhibition of Plasmodium falciparum choline kinase by hexadecyltrimethylammonium bromide: a possible antimalarial mechanism. Antimicrob Agents Chemother **51:**696-706.

29. **Conway, D. J.** 2007. Molecular epidemiology of malaria. Clin Microbiol Rev **20:**188-204.

30. **Cook, J. A., E. J. Randinitis, C. R. Bramson, and D. L. Wesche.** 2006. Lack of a pharmacokinetic interaction between azithromycin and chloroquine. Am J Trop Med Hyg **74:**407-12.

31. **Cooper, R. A., C. L. Hartwig, and M. T. Ferdig.** 2005. pfcrt is more than the Plasmodium falciparum chloroquine resistance gene: a functional and evolutionary perspective. Acta Trop **94:**170-80.

32. **Cory, M., R. R. Tidwell, and T. A. Fairley.** 1992. Structure and DNA binding activity of analogues of 1,5-bis(4-amidinophenoxy)pentane (pentamidine). J Med Chem **35:**431-8.

33. **Cowman, A. F.** 1991. The P-glycoprotein homologues of Plasmodium falciparum: Are they involved in chloroquine resistance? Parasitol Today **7:**70-6.

34. **Cowman, A. F., D. Galatis, and J. K. Thompson.** 1994. Selection for mefloquine resistance in Plasmodium falciparum is linked to amplification of the pfmdr1 gene and cross-resistance to halofantrine and quinine. Proc Natl Acad Sci U S A **91:**1143-7.

35. **Crabb, B. S., and A. F. Cowman.** 2002. Plasmodium falciparum virulence determinants unveiled. Genome Biol **3:**REVIEWS1031.

36. **Dahl, E. L., and P. J. Rosenthal.** 2007. Multiple antibiotics exert delayed effects against the Plasmodium falciparum apicoplast. Antimicrob Agents Chemother **51:**3485-90.

37. **Daily, J. P.** 2006. Antimalarial Drug Therapy: The Role of Parasite Biology and Drug Resistance. J Clin Pharmacol **46:**1487-1497.

38. **Daroff, R. B., J. J. Deller, Jr., A. J. Kastl, Jr., and W. Blocker, Jr.** 1967. Cerebral malaria. Jama **202:**679-82.

39. **de Monbrison, F., D. Raynaud, C. Latour-Fondanaiche, A. Staal, S. Favre, K. Kaiser, F. Peyron, and S. Picot.** 2003. Real-time PCR for chloroquine sensitivity assay and for pfmdr1-pfcrt single nucleotide polymorphisms in Plasmodium falciparum. J Microbiol Methods **54:**391-401.

40. **Desai, S. A.** 2004. Targeting ion channels of Plasmodium falciparum-infected human erythrocytes for antimalarial development. Curr Drug Targets Infect Disord **4:**79-86.

41. **Desjardins, R. E., C. J. Canfield, J. D. Haynes, and J. D. Chulay.** 1979. Quantitative assessment of antimalarial activity in vitro by a semiautomated microdilution technique. Antimicrob Agents Chemother **16:**710-8.

42. **Djimde, A., O. K. Doumbo, J. F. Cortese, K. Kayentao, S. Doumbo, Y. Diourte, A. Dicko, X. Z. Su, T. Nomura, D. A. Fidock, T. E. Wellems, C. V. Plowe, and D. Coulibaly.** 2001. A molecular marker for chloroquine-resistant falciparum malaria. N Engl J Med **344:**257-63.

43. **Dokomajilar, C., Z. M. Lankoande, G. Dorsey, I. Zongo, J. B. Ouedraogo, and P. J. Rosenthal.** 2006. Roles of specific Plasmodium falciparum mutations in resistance to amodiaquine and sulfadoxine-pyrimethamine in Burkina Faso. Am J Trop Med Hyg **75:**162-5.

44. **Duah, N. O., M. D. Wilson, A. Ghansah, B. Abuaku, D. Edoh, N. B. Quashie, and K. A. Koram.** 2007. Mutations in Plasmodium falciparum chloroquine resistance

transporter and multidrug resistance genes, and treatment outcomes in Ghanaian children with uncomplicated malaria. J Trop Pediatr **53:**27-31.

45. **Duraisingh, M. T., and A. F. Cowman.** 2005. Contribution of the pfmdr1 gene to antimalarial drug-resistance. Acta Trop **94:**181-90.

46. **Duraisingh, M. T., C. J. Drakeley, O. Muller, R. Bailey, G. Snounou, G. A. Targett, B. M. Greenwood, and D. C. Warhurst.** 1997. Evidence for selection for the tyrosine-86 allele of the pfmdr 1 gene of Plasmodium falciparum by chloroquine and amodiaquine. Parasitology **114 (Pt 3):**205-11.

47. **Duraisingh, M. T., P. Jones, I. Sambou, L. von Seidlein, M. Pinder, and D. C. Warhurst.** 2000. The tyrosine-86 allele of the pfmdr1 gene of Plasmodium falciparum is associated with increased sensitivity to the anti-malarials mefloquine and artemisinin. Mol Biochem Parasitol **108:**13-23.

48. **Duraisingh, M. T., C. Roper, D. Walliker, and D. C. Warhurst.** 2000. Increased sensitivity to the antimalarials mefloquine and artemisinin is conferred by mutations in the pfmdr1 gene of Plasmodium falciparum. Mol Microbiol **36:**955-61.

49. **Eckstein-Ludwig, U., R. J. Webb, I. D. Van Goethem, J. M. East, A. G. Lee, M. Kimura, P. M. O'Neill, P. G. Bray, S. A. Ward, and S. Krishna.** 2003. Artemisinins target the SERCA of Plasmodium falciparum. Nature **424:**957-61.

50. **Eline Korenromp, J. M., Bernard Nahlen, Tessa Wardlaw and Mark Young.** 2005. World Malaria Report 2005. World Health Organization.

51. **English, M., R. Sauerwein, C. Waruiru, M. Mosobo, J. Obiero, B. Lowe, and K. Marsh.** 1997. Acidosis in severe childhood malaria. Qjm **90:**263-70.

52. **Feddersen, A., and K. Sack.** 1991. Experimental studies on the nephrotoxicity of pentamidine in rats. J Antimicrob Chemother **28:**437-46.

53. **Fichera, M. E., and D. S. Roos.** 1997. A plastid organelle as a drug target in apicomplexan parasites. Nature **390:**407-9.

54. **Fidock, D. A., T. Nomura, A. K. Talley, R. A. Cooper, S. M. Dzekunov, M. T. Ferdig, L. M. Ursos, A. B. Sidhu, B. Naude, K. W. Deitsch, X. Z. Su, J. C. Wootton, P. D. Roepe, and T. E. Wellems.** 2000. Mutations in the P. falciparum digestive vacuole transmembrane protein PfCRT and evidence for their role in chloroquine resistance. Mol Cell **6:**861-71.

55. **Fitch, C. D., and N. V. Russell.** 2006. Accelerated denaturation of hemoglobin and the antimalarial action of chloroquine. Antimicrob Agents Chemother **50:**2415-9.

56. **Foote, S. J., D. E. Kyle, R. K. Martin, A. M. Oduola, K. Forsyth, D. J. Kemp, and A. F. Cowman.** 1990. Several alleles of the multidrug-resistance gene are closely linked to chloroquine resistance in Plasmodium falciparum. Nature **345:**255-8.

57. **Gardner, M. J., N. Hall, E. Fung, O. White, M. Berriman, R. W. Hyman, J. M. Carlton, A. Pain, K. E. Nelson, S. Bowman, I. T. Paulsen, K. James, J. A. Eisen, K. Rutherford, S. L. Salzberg, A. Craig, S. Kyes, M. S. Chan, V. Nene, S. J. Shallom, B. Suh, J. Peterson, S. Angiuoli, M. Pertea, J. Allen, J. Selengut, D. Haft, M. W. Mather, A. B. Vaidya, D. M. Martin, A. H. Fairlamb, M. J. Fraunholz, D. S. Roos, S. A. Ralph, G. I. McFadden, L. M. Cummings, G. M. Subramanian, C. Mungall, J. C. Venter, D. J. Carucci, S. L. Hoffman, C. Newbold, R. W. Davis, C. M. Fraser, and B. Barrell.** 2002. Genome sequence of the human malaria parasite Plasmodium falciparum. Nature **419:**498-511.

58. **Gay, F., D. G. Bustos, B. Diquet, L. Rojas Rivero, M. Litaudon, C. Pichet, M. Danis, and M. Gentilini.** 1990. Cross-resistance between mefloquine and halofantrine. Lancet **336:**1262.

59. **Geary, T. G., A. A. Divo, and J. B. Jensen.** 1988. Uptake of antibiotics by Plasmodium falciparum in culture. Am J Trop Med Hyg **38:**466-9.

60. **Gritzmacher, C. A., and R. T. Reese.** 1984. Protein and nucleic acid synthesis during synchronized growth of Plasmodium falciparum. J. Bacteriol. **160:**1165-1167.

61. **Grobusch, M. P., and P. G. Kremsner.** 2005. Uncomplicated malaria. Curr Top Microbiol Immunol **295:**83-104.

62. **Happi, C. T., G. O. Gbotosho, O. A. Folarin, O. M. Bolaji, A. Sowunmi, D. E. Kyle, W. Milhous, D. F. Wirth, and A. M. Oduola.** 2006. Association between mutations in Plasmodium falciparum chloroquine resistance transporter and P. falciparum multidrug resistance 1 genes and in vivo amodiaquine resistance in P. falciparum malaria-infected children in Nigeria. Am J Trop Med Hyg **75:**155-61.

63. **Happi, T. C., S. M. Thomas, G. O. Gbotosho, C. O. Falade, D. O. Akinboye, L. Gerena, T. Hudson, A. Sowunmi, D. E. Kyle, W. Milhous, D. F. Wirth, and A. M. Oduola.** 2003. Point mutations in the pfcrt and pfmdr-1 genes of Plasmodium falciparum and clinical response to chloroquine, among malaria patients from Nigeria. Ann Trop Med Parasitol **97:**439-51.

64. **Hastings, I. M., W. M. Watkins, and N. J. White.** 2002. The evolution of drug-resistant malaria: the role of drug elimination half-life. Philos Trans R Soc Lond B Biol Sci **357:**505-19.

65. **Holland, P. M., R. D. Abramson, R. Watson, and D. H. Gelfand.** 1991. Detection of specific polymerase chain reaction product by utilizing the 5'----3' exonuclease

activity of Thermus aquaticus DNA polymerase. Proc Natl Acad Sci U S A **88:**7276-80.

66. **Holmgren, G., J. Hamrin, J. Svard, A. Martensson, J. P. Gil, and A. Bjorkman.** 2007. Selection of pfmdr1 mutations after amodiaquine monotherapy and amodiaquine plus artemisinin combination therapy in East Africa. Infect Genet Evol.

67. **Humphreys, G. S., I. Merinopoulos, J. Ahmed, C. J. Whitty, T. K. Mutabingwa, C. J. Sutherland, and R. L. Hallett.** 2007. Amodiaquine and artemether-lumefantrine select distinct alleles of the Plasmodium falciparum mdr1 gene in Tanzanian children treated for uncomplicated malaria. Antimicrob Agents Chemother **51:**991-7.

68. **Hung le, Q., P. J. de Vries, T. Q. Binh, P. T. Giao, N. V. Nam, R. Holman, and P. A. Kager.** 2004. Artesunate with mefloquine at various intervals for non-severe Plasmodium falciparum malaria. Am J Trop Med Hyg **71:**160-6.

69. **Hussein, Z., J. Eaves, D. B. Hutchinson, and C. J. Canfield.** 1997. Population pharmacokinetics of atovaquone in patients with acute malaria caused by Plasmodium falciparum. Clin Pharmacol Ther **61:**518-30.

70. **Inselburg, J., and H. S. Banyal.** 1984. Plasmodium falciparum: synchronization of asexual development with aphidicolin, a DNA synthesis inhibitor. Exp Parasitol **57:**48-54.

71. **Jiang, H., D. A. Joy, T. Furuya, and X. Z. Su.** 2006. Current understanding of the molecular basis of chloroquine-resistance in Plasmodium falciparum. J Postgrad Med **52:**271-6.

72. **Juliano, J. J., J. J. Kwiek, K. Cappell, V. Mwapasa, and S. R. Meshnick.** 2007. Minority-variant pfcrt K76T mutations and chloroquine resistance, Malawi. Emerg Infect Dis **13:**872-7.

73. **Juliano, R. L., and V. Ling.** 1976. A surface glycoprotein modulating drug permeability in Chinese hamster ovary cell mutants. Biochim Biophys Acta **455:**152-62.

74. **Kelly, J. X., R. W. Winter, A. Cornea, D. H. Peyton, D. J. Hinrichs, and M. Riscoe.** 2002. The kinetics of uptake and accumulation of 3,6-bis-omega-diethylamino-amyloxyxanthone by the human malaria parasite Plasmodium falciparum. Mol Biochem Parasitol **123:**47-54.

75. **Khim, N., C. Bouchier, M. T. Ekala, S. Incardona, P. Lim, E. Legrand, R. Jambou, S. Doung, O. M. Puijalon, and T. Fandeur.** 2005. Countrywide survey shows very high prevalence of Plasmodium falciparum multilocus resistance genotypes in Cambodia. Antimicrob Agents Chemother **49:**3147-52.

76. **Kirk, K.** 2000. Malaria. Channelling nutrients. Nature **406:**949, 951.

77. **Kirk, K.** 2001. Membrane Transport in the Malaria-Infected Erythrocyte. Physiol. Rev. **81:**495-537.

78. **Kirk, K., H. A. Horner, B. C. Elford, J. C. Ellory, and C. I. Newbold.** 1994. Transport of diverse substrates into malaria-infected erythrocytes via a pathway showing functional characteristics of a chloride channel. J Biol Chem **269:**3339-47.

79. **Kokwaro, G., L. Mwai, and A. Nzila.** 2007. Artemether/lumefantrine in the treatment of uncomplicated falciparum malaria. Expert Opin Pharmacother **8:**75-94.

80. **Krishna, S., S. Pukrittayakamee, W. Supanaranond, F. ter Kuile, M. Ruprah, T. Sura, and N. J. White.** 1995. Fever in uncomplicated Plasmodium falciparum malaria: randomized double-'blind' comparison of ibuprofen and paracetamol treatment. Trans R Soc Trop Med Hyg **89:**507-9.

81. **Krishna, S., W. Supanaranond, S. Pukrittayakamee, F. ter Kuile, Y. Supputamangkol, K. Attatamsoonthorn, M. Ruprah, and N. J. White.** 1995. Fever in uncomplicated Plasmodium falciparum infection: effects of quinine and paracetamol. Trans R Soc Trop Med Hyg **89:**197-9.

82. **Krudsood, S., S. N. Patel, N. Tangpukdee, W. Thanachartwet, W. Leowattana, K. Pornpininworakij, A. K. Boggild, S. Looareesuwan, and K. C. Kain.** 2007. EFFICACY OF ATOVAQUONE-PROGUANIL FOR TREATMENT OF ACUTE MULTIDRUG-RESISTANT PLASMODIUM FALCIPARUM MALARIA IN THAILAND. Am J Trop Med Hyg **76:**655-658.

83. **Lakshmanan, V., P. G. Bray, D. Verdier-Pinard, D. J. Johnson, P. Horrocks, R. A. Muhle, G. E. Alakpa, R. H. Hughes, S. A. Ward, D. J. Krogstad, A. B. Sidhu, and D. A. Fidock.** 2005. A critical role for PfCRT K76T in Plasmodium falciparum verapamil-reversible chloroquine resistance. Embo J **24:**2294-305.

84. **Lambros, C., and J. P. Vanderberg.** 1979. Synchronization of Plasmodium falciparum erythrocytic stages in culture. J Parasitol **65:**418-20.

85. **Lansiaux, A., F. Tanious, Z. Mishal, L. Dassonneville, A. Kumar, C. E. Stephens, Q. Hu, W. D. Wilson, D. W. Boykin, and C. Bailly.** 2002. Distribution of furamidine analogues in tumor cells: targeting of the nucleus or mitochondria depending on the amidine substitution. Cancer Res **62:**7219-29.

86. **Lanteri, C. A., B. L. Trumpower, R. R. Tidwell, and S. R. Meshnick.** 2004. DB75, a novel trypanocidal agent, disrupts mitochondrial function in Saccharomyces cerevisiae. Antimicrob Agents Chemother **48:**3968-74.

87. **Lauer, S. A., P. K. Rathod, N. Ghori, and K. Haldar.** 1997. A membrane network for nutrient import in red cells infected with the malaria parasite. Science **276:**1122-5.

88. **Le Bras, J., and R. Durand.** 2003. The mechanisms of resistance to antimalarial drugs in Plasmodium falciparum. Fundam Clin Pharmacol **17:**147-53.

89. **Le Roch, K. G., J. R. Johnson, L. Florens, Y. Zhou, A. Santrosyan, M. Grainger, S. F. Yan, K. C. Williamson, A. A. Holder, D. J. Carucci, J. R. Yates, III, and E. A. Winzeler.** 2004. Global analysis of transcript and protein levels across the Plasmodium falciparum life cycle. Genome Res. **14:**2308-2318.

90. **Livak, K. J.** 1999. Allelic discrimination using fluorogenic probes and the 5' nuclease assay. Genet Anal **14:**143-9.

91. **Macreadie, I., H. Ginsburg, W. Sirawaraporn, and L. Tilley.** 2000. Antimalarial drug development and new targets. Parasitol Today **16:**438-44.

92. **Marchesini, N., S. Luo, C. O. Rodrigues, S. N. Moreno, and R. Docampo.** 2000. Acidocalcisomes and a vacuolar H+-pyrophosphatase in malaria parasites. Biochem J **347 Pt 1:**243-53.

93. **Marini, J. C., P. N. Effron, T. C. Goodman, C. K. Singleton, R. D. Wells, R. M. Wartell, and P. T. Englund.** 1984. Physical characterization of a kinetoplast DNA fragment with unusual properties. J Biol Chem **259:**8974-9.

94. **Marsh, K., D. Forster, C. Waruiru, I. Mwangi, M. Winstanley, V. Marsh, C. Newton, P. Winstanley, P. Warn, N. Peshu, and et al.** 1995. Indicators of life-threatening malaria in African children. N Engl J Med **332:**1399-404.

95. **Martin, R. M., H. Leonhardt, and M. C. Cardoso.** 2005. DNA labeling in living cells. Cytometry A **67:**45-52.

96. **Mathis, A. M., A. S. Bridges, M. A. Ismail, A. Kumar, I. Francesconi, M. Anbazhagan, Q. Hu, F. A. Tanious, T. Wenzler, J. Saulter, W. D. Wilson, R. Brun, D. W. Boykin, R. R. Tidwell, and J. E. Hall.** 2007. Diphenyl furans and aza analogs: effects of structural modification on in vitro activity, DNA binding, and accumulation and distribution in trypanosomes. Antimicrob Agents Chemother **51:**2801-10.

97. **Mathis, A. M., J. L. Holman, L. M. Sturk, M. A. Ismail, D. W. Boykin, R. R. Tidwell, and J. E. Hall.** 2006. Accumulation and intracellular distribution of antitrypanosomal diamidine compounds DB75 and DB820 in African trypanosomes. Antimicrob Agents Chemother **50:**2185-91.

98. **Mazur, S., F. A. Tanious, D. Ding, A. Kumar, D. W. Boykin, I. J. Simpson, S. Neidle, and W. D. Wilson.** 2000. A thermodynamic and structural analysis of DNA minor-groove complex formation. J Mol Biol **300:**321-37.

99. **Menard, D., F. Yapou, A. Manirakiza, D. Djalle, M. D. Matsika-Claquin, and A. Talarmin.** 2006. Polymorphisms in pfcrt, pfmdr1, dhfr genes and in vitro responses to antimalarials in Plasmodium falciparum isolates from Bangui, Central African Republic. Am J Trop Med Hyg **75:**381-7.

100. **Meshnick, S. R., T. E. Taylor, and S. Kamchonwongpaisan.** 1996. Artemisinin and the antimalarial endoperoxides: from herbal remedy to targeted chemotherapy. Microbiol. Rev. **60:**301-315.

101. **Meshnick, S. R., A. Thomas, A. Ranz, C. M. Xu, and H. Z. Pan.** 1991. Artemisinin (qinghaosu): the role of intracellular hemin in its mechanism of antimalarial action. Mol Biochem Parasitol **49:**181-9.

102. **Mishra, S. K., S. Mohanty, A. Mohanty, and B. S. Das.** 2006. Management of severe and complicated malaria. J Postgrad Med **52:**281-7.

103. **Morty, R. E., L. Troeberg, R. N. Pike, R. Jones, P. Nickel, J. D. Lonsdale-Eccles, and T. H. Coetzer.** 1998. A trypanosome oligopeptidase as a target for the trypanocidal agents pentamidine, diminazene and suramin. FEBS Lett **433:**251-6.

104. **Nelson, A. L., A. Purfield, P. McDaniel, N. Uthaimongkol, N. Buathong, S. Sriwichai, R. S. Miller, C. Wongsrichanalai, and S. R. Meshnick.** 2005. pfmdr1 genotyping and in vivo mefloquine resistance on the Thai-Myanmar border. Am J Trop Med Hyg **72:**586-92.

105. **Nguyen, B., C. Tardy, C. Bailly, P. Colson, C. Houssier, A. Kumar, D. W. Boykin, and W. D. Wilson.** 2002. Influence of compound structure on affinity, sequence selectivity, and mode of binding to DNA for unfused aromatic dications related to furamidine. Biopolymers **63:**281-97.

106. **Nkhoma, S., M. Molyneux, and S. Ward.** 2007. In vitro antimalarial susceptibility profile and prcrt/pfmdr-1 genotypes of Plasmodium falciparum field isolates from Malawi. Am J Trop Med Hyg **76:**1107-12.

107. **Nsobya, S. L., C. Dokomajilar, M. Joloba, G. Dorsey, and P. J. Rosenthal.** 2007. Resistance-Mediating Plasmodium falciparum pfcrt and pfmdr1 Alleles after Treatment with Artesunate-Amodiaquine in Uganda. Antimicrob Agents Chemother **51:**3023-5.

108. **Oduola, A. M., W. K. Milhous, N. F. Weatherly, J. H. Bowdre, and R. E. Desjardins.** 1988. Plasmodium falciparum: induction of resistance to mefloquine in cloned strains by continuous drug exposure in vitro. Exp Parasitol **67:**354-60.

109. **Ojurongbe, O., T. O. Ogungbamigbe, A. F. Fagbenro-Beyioku, R. Fendel, P. G. Kremsner, and J. F. Kun.** 2007. Rapid detection of Pfcrt and Pfmdr1 mutations in Plasmodium falciparum isolates by FRET and in vivo response to chloroquine among children from Osogbo, Nigeria. Malar J **6:**41.

110. **Olliaro, P.** 2001. Mode of action and mechanisms of resistance for antimalarial drugs. Pharmacol Ther **89:**207-19.

111. **Peel, S. A., P. Bright, B. Yount, J. Handy, and R. S. Baric.** 1994. A strong association between mefloquine and halofantrine resistance and amplification, overexpression, and mutation in the P-glycoprotein gene homolog (pfmdr) of Plasmodium falciparum in vitro. Am J Trop Med Hyg **51:**648-58.

112. **Petersen, T. W., S. F. Ibrahim, A. H. Diercks, and G. van den Engh.** 2004. Chromatic shifts in the fluorescence emitted by murine thymocytes stained with Hoechst 33342. Cytometry A **60:**173-81.

113. **Pfaffl, M. W.** 2001. A new mathematical model for relative quantification in real-time RT-PCR. Nucleic Acids Res **29:**e45.

114. **Pickard, A. L., C. Wongsrichanalai, A. Purfield, D. Kamwendo, K. Emery, C. Zalewski, F. Kawamoto, R. S. Miller, and S. R. Meshnick.** 2003. Resistance to antimalarials in Southeast Asia and genetic polymorphisms in pfmdr1. Antimicrob Agents Chemother **47:**2418-23.

115. **Pillai, D. R., G. Hijar, Y. Montoya, W. Marouino, T. K. Ruebush, 2nd, C. Wongsrichanalai, and K. C. Kain.** 2003. Lack of prediction of mefloquine and mefloquine-artesunate treatment outcome by mutations in the Plasmodium falciparum multidrug resistance 1 (pfmdr1) gene for P. falciparum malaria in Peru. Am J Trop Med Hyg **68:**107-10.

116. **Planche, T., A. Dzeing, E. Ngou-Milama, M. Kombila, and P. W. Stacpoole.** 2005. Metabolic complications of severe malaria. Curr Top Microbiol Immunol **295:**105-36.

117. **Plowe, C. V.** 2003. Monitoring antimalarial drug resistance: making the most of the tools at hand. J Exp Biol **206:**3745-52.

118. **Price, R. N., C. Cassar, A. Brockman, M. Duraisingh, M. van Vugt, N. J. White, F. Nosten, and S. Krishna.** 1999. The pfmdr1 gene is associated with a multidrug-resistant phenotype in Plasmodium falciparum from the western border of Thailand. Antimicrob Agents Chemother **43:**2943-9.

119. **Price, R. N., F. Nosten, C. Luxemburger, A. Kham, A. Brockman, T. Chongsuphajaisiddhi, and N. J. White.** 1995. Artesunate versus artemether in

combination with mefloquine for the treatment of multidrug-resistant falciparum malaria. Trans R Soc Trop Med Hyg **89:**523-7.

120. **Price, R. N., A. C. Uhlemann, A. Brockman, R. McGready, E. Ashley, L. Phaipun, R. Patel, K. Laing, S. Looareesuwan, N. J. White, F. Nosten, and S. Krishna.** 2004. Mefloquine resistance in Plasmodium falciparum and increased pfmdr1 gene copy number. Lancet **364:**438-47.

121. **Purfield, A., A. Nelson, A. Laoboonchai, K. Congpuong, P. McDaniel, R. S. Miller, K. Welch, C. Wongsrichanalai, and S. R. Meshnick.** 2004. A new method for detection of pfmdr1 mutations in Plasmodium falciparum DNA using real-time PCR. Malar J **3:**9.

122. **Rahmathullah, S. M., J. E. Hall, B. C. Bender, D. R. McCurdy, R. R. Tidwell, and D. W. Boykin.** 1999. Prodrugs for amidines: synthesis and anti-Pneumocystis carinii activity of carbamates of 2,5-bis(4-amidinophenyl)furan. J Med Chem **42:**3994-4000.

123. **Ramya, T. N., S. Mishra, K. Karmodiya, N. Surolia, and A. Surolia.** 2007. Inhibitors of nonhousekeeping functions of the apicoplast defy delayed death in Plasmodium falciparum. Antimicrob Agents Chemother **51:**307-16.

124. **Reed, M. B., K. J. Saliba, S. R. Caruana, K. Kirk, and A. F. Cowman.** 2000. Pgh1 modulates sensitivity and resistance to multiple antimalarials in Plasmodium falciparum. Nature **403:**906-9.

125. **Ringwald, P., and L. K. Basco.** 1999. Comparison of in vivo and in vitro tests of resistance in patients treated with chloroquine in Yaounde, Cameroon. Bull World Health Organ **77:**34-43.

126. **Rohrbach, P., C. P. Sanchez, K. Hayton, O. Friedrich, J. Patel, A. B. Sidhu, M. T. Ferdig, D. A. Fidock, and M. Lanzer.** 2006. Genetic linkage of pfmdr1 with food vacuolar solute import in Plasmodium falciparum. Embo J **25:**3000-11.

127. **Rojanawatsirivet, C., K. Congpuong, S. Vijaykadga, S. Thongphua, K. Thongsri, K. N. Bangchang, P. Wilairatana, and W. H. Wernsdorfer.** 2004. Declining mefloquine sensitivity of Plasmodium falciparum along the Thai-Myanmar border. Southeast Asian J Trop Med Public Health **35:**560-5.

128. **Roninson, I. B.** 1992. The role of the MDR1 (P-glycoprotein) gene in multidrug resistance in vitro and in vivo. Biochem Pharmacol **43:**95-102.

129. **Rosypal, A. C., J. E. Hall, S. Bakunova, D. A. Patrick, S. Bakunov, C. E. Stephens, A. Kumar, D. W. Boykin, and R. R. Tidwell.** In vitro activity of dicationic compounds against a North American foxhound isolate of Leishmania infantum. Veterinary Parasitology **In Press, Corrected Proof**.

130. **Rowe, A. K., S. Y. Rowe, R. W. Snow, E. L. Korenromp, J. R. M. A. Schellenberg, C. Stein, B. L. Nahlen, J. Bryce, R. E. Black, and R. W. Steketee.** 2006. The burden of malaria mortality among African children in the year 2000. Int. J. Epidemiol. **35:**691-704.

131. **Sanchez, C. P., J. E. McLean, P. Rohrbach, D. A. Fidock, W. D. Stein, and M. Lanzer.** 2005. Evidence for a pfcrt-associated chloroquine efflux system in the human malarial parasite Plasmodium falciparum. Biochemistry **44:**9862-70.

132. **Sanchez, C. P., W. Stein, and M. Lanzer.** 2003. Trans stimulation provides evidence for a drug efflux carrier as the mechanism of chloroquine resistance in Plasmodium falciparum. Biochemistry **42:**9383-94.

133. **Sands, M., M. A. Kron, and R. B. Brown.** 1985. Pentamidine: a review. Rev Infect Dis **7:**625-34.

134. **Sato, S., and R. J. Wilson.** 2005. The plastid of Plasmodium spp.: a target for inhibitors. Curr Top Microbiol Immunol **295:**251-73.

135. **Saulter, J. Y., J. R. Kurian, L. A. Trepanier, R. R. Tidwell, A. S. Bridges, D. W. Boykin, C. E. Stephens, M. Anbazhagan, and J. E. Hall.** 2005. Unusual dehydroxylation of antimicrobial amidoxime prodrugs by cytochrome b5 and NADH cytochrome b5 reductase. Drug Metab Dispos **33:**1886-93.

136. **Schellenberg, D., C. Menendez, E. Kahigwa, F. Font, C. Galindo, C. Acosta, J. A. Schellenberg, J. J. Aponte, J. Kimario, H. Urassa, H. Mshinda, M. Tanner, and P. Alonso.** 1999. African children with malaria in an area of intense Plasmodium falciparum transmission: features on admission to the hospital and risk factors for death. Am J Trop Med Hyg **61:**431-8.

137. **Seaberg, L. S., A. R. Parquette, I. Y. Gluzman, G. W. Phillips, Jr., T. F. Brodasky, and D. J. Krogstad.** 1984. Clindamycin activity against chloroquine-resistant Plasmodium falciparum. J Infect Dis **150:**904-11.

138. **Segurado, A. A., S. M. di Santi, and M. Shiroma.** 1997. In vivo and in vitro Plasmodium falciparum resistance to chloroquine, amodiaquine and quinine in the Brazilian Amazon. Rev Inst Med Trop Sao Paulo **39:**85-90.

139. **Seow, F., S. Sato, C. S. Janssen, M. O. Riehle, A. Mukhopadhyay, R. S. Phillips, R. J. Wilson, and M. P. Barrett.** 2005. The plastidic DNA replication enzyme complex of Plasmodium falciparum. Mol Biochem Parasitol **141:**145-153.

140. **Sibley, C. H., and P. Ringwald.** 2006. A database of antimalarial drug resistance. Malar J **5:**48.

141. **Sidhu, A. B., D. Verdier-Pinard, and D. A. Fidock.** 2002. Chloroquine resistance in Plasmodium falciparum malaria parasites conferred by pfcrt mutations. Science **298:**210-3.

142. **Silamut, K., and N. J. White.** 1993. Relation of the stage of parasite development in the peripheral blood to prognosis in severe falciparum malaria. Trans R Soc Trop Med Hyg **87:**436-43.

143. **Sinden, R. E.** 2002. Molecular interactions between Plasmodium and its insect vectors. Cell Microbiol **4:**713-24.

144. **Sisowath, C., P. E. Ferreira, L. Y. Bustamante, S. Dahlstrom, A. Martensson, A. Bjorkman, S. Krishna, and J. P. Gil.** 2007. The role of pfmdr1 in Plasmodium falciparum tolerance to artemether-lumefantrine in Africa. Trop Med Int Health **12:**736-42.

145. **Skudowitz, R. B., J. Katz, A. Lurie, J. Levin, and J. Metz.** 1973. Mechanisms of thrombocytopenia in malignant tertian malaria. Br Med J **2:**515-8.

146. **Snow, R. W., C. A. Guerra, A. M. Noor, H. Y. Myint, and S. I. Hay.** 2005. The global distribution of clinical episodes of Plasmodium falciparum malaria. Nature **434:**214-217.

147. **Stead, A. M., P. G. Bray, I. G. Edwards, H. P. DeKoning, B. C. Elford, P. A. Stocks, and S. A. Ward.** 2001. Diamidine compounds: selective uptake and targeting in Plasmodium falciparum. Mol Pharmacol **59:**1298-306.

148. **Steele, R. W.** 1996. Malaria in children. Adv Pediatr Infect Dis **12:**325-49.

149. **Steele, R. W., and B. Baffoe-Bonnie.** 1995. Cerebral malaria in children. Pediatr Infect Dis J **14:**281-5.

150. **Sullivan, D. J., Jr., I. Y. Gluzman, D. G. Russell, and D. E. Goldberg.** 1996. On the molecular mechanism of chloroquine's antimalarial action. Proceedings of the National Academy of Sciences **93:**11865-11870.

151. **Takechi, M., M. Matsuo, C. Ziba, A. MacHeso, D. Butao, I. L. Zungu, I. Chakanika, and M. D. Bustos.** 2001. Therapeutic efficacy of sulphadoxine/pyrimethamine and susceptibility in vitro of P. falciparum isolates to sulphadoxine-pyremethamine and other antimalarial drugs in Malawian children. Trop Med Int Health **6:**429-34.

152. **Talisuna, A. O., P. Bloland, and U. D'Alessandro.** 2004. History, dynamics, and public health importance of malaria parasite resistance. Clin Microbiol Rev **17:**235-54.

153. **Tidwell, R. R., S. K. Jones, J. D. Geratz, K. A. Ohemeng, C. A. Bell, B. J. Berger, and J. E. Hall.** 1990. Development of pentamidine analogues as new agents for the treatment of Pneumocystis carinii pneumonia. Ann N Y Acad Sci **616:**421-41.

154. **Tinto, H., J. B. Ouedraogo, A. Erhart, C. Van Overmeir, J. C. Dujardin, E. Van Marck, T. R. Guiguemde, and U. D'Alessandro.** 2003. Relationship between the Pfcrt T76 and the Pfmdr-1 Y86 mutations in Plasmodium falciparum and in vitro/in vivo chloroquine resistance in Burkina Faso, West Africa. Infect Genet Evol **3:**287-92.

155. **Trager, W., and J. B. Jensen.** 1976. Human malaria parasites in continuous culture. Science **193:**673-5.

156. **Uhlemann, A. C., A. Cameron, U. Eckstein-Ludwig, J. Fischbarg, P. Iserovich, F. A. Zuniga, M. East, A. Lee, L. Brady, R. K. Haynes, and S. Krishna.** 2005. A single amino acid residue can determine the sensitivity of SERCAs to artemisinins. Nat Struct Mol Biol **12:**628-9.

157. **van Es, H. H., S. Karcz, F. Chu, A. F. Cowman, S. Vidal, P. Gros, and E. Schurr.** 1994. Expression of the plasmodial pfmdr1 gene in mammalian cells is associated with increased susceptibility to chloroquine. Mol Cell Biol **14:**2419-28.

158. **Vercesi, A. E., and R. Docampo.** 1992. Ca2+ transport by digitonin-permeabilized Leishmania donovani. Effects of Ca2+, pentamidine and WR-6026 on mitochondrial membrane potential in situ. Biochem J **284 (Pt 2):**463-7.

159. **Viriyakosol, S., N. Siripoon, X. P. Zhu, W. Jarra, A. Seugorn, K. N. Brown, and G. Snounou.** 1994. Plasmodium falciparum: selective growth of subpopulations from field samples following in vitro culture, as detected by the polymerase chain reaction. Exp Parasitol **79:**517-25.

160. **Volkman, S., and D. Wirth.** 1998. Functional analysis of pfmdr1 gene of Plasmodium falciparum. Methods Enzymol **292:**174-81.

161. **Waller, K. L., R. A. Muhle, L. M. Ursos, P. Horrocks, D. Verdier-Pinard, A. B. Sidhu, H. Fujioka, P. D. Roepe, and D. A. Fidock.** 2003. Chloroquine resistance modulated in vitro by expression levels of the Plasmodium falciparum chloroquine resistance transporter. J Biol Chem **278:**33593-601.

162. **Wang, M. Z., J. Y. Saulter, E. Usuki, Y. L. Cheung, M. Hall, A. S. Bridges, G. Loewen, O. T. Parkinson, C. E. Stephens, J. L. Allen, D. C. Zeldin, D. W. Boykin, R. R. Tidwell, A. Parkinson, M. F. Paine, and J. E. Hall.** 2006. CYP4F enzymes are the major enzymes in human liver microsomes that catalyze the O-demethylation of the antiparasitic prodrug DB289 [2,5-bis(4-amidinophenyl)furan-bis-O-methylamidoxime]. Drug Metab Dispos **34:**1985-94.

163. **Watkins, W. M., and M. Mosobo.** 1993. Treatment of Plasmodium falciparum malaria with pyrimethamine-sulfadoxine: selective pressure for resistance is a function of long elimination half-life. Trans R Soc Trop Med Hyg **87:**75-8.

164. **Webster, H. K., E. F. Boudreau, K. Pavanand, K. Yongvanitchit, and L. W. Pang.** 1985. Antimalarial drug susceptibility testing of Plasmodium falciparum in Thailand using a microdilution radioisotope method. Am J Trop Med Hyg **34:**228-35.

165. **Werbovetz, K.** 2006. Diamidines as antitrypanosomal, antileishmanial and antimalarial agents. Curr Opin Investig Drugs **7:**147-57.

166. **Wernsdorfer, W. H., and H. Noedl.** 2003. Molecular markers for drug resistance in malaria: use in treatment, diagnosis and epidemiology. Curr Opin Infect Dis **16:**553-8.

167. **White, N. J.** 2004. Antimalarial drug resistance. J Clin Invest **113:**1084-92.

168. **White, N. J.** 1999. Delaying antimalarial drug resistance with combination chemotherapy. Parassitologia **41:**301-8.

169. **White, N. J., and P. L. Olliaro.** 1996. Strategies for the prevention of antimalarial drug resistance: rationale for combination chemotherapy for malaria. Parasitol Today **12:**399-401.

170. **Wilson, C. M., A. E. Serrano, A. Wasley, M. P. Bogenschutz, A. H. Shankar, and D. F. Wirth.** 1989. Amplification of a gene related to mammalian mdr genes in drug-resistant Plasmodium falciparum. Science **244:**1184-6.

171. **Wilson, C. M., S. K. Volkman, S. Thaithong, R. K. Martin, D. E. Kyle, W. K. Milhous, and D. F. Wirth.** 1993. Amplification of pfmdr 1 associated with mefloquine and halofantrine resistance in Plasmodium falciparum from Thailand. Mol Biochem Parasitol **57:**151-60.

172. **Wongsrichanalai, C., A. L. Pickard, W. H. Wernsdorfer, and S. R. Meshnick.** 2002. Epidemiology of drug-resistant malaria. Lancet Infect Dis **2:**209-18.

173. **Woodrow, C. J., R. K. Haynes, and S. Krishna.** 2005. Artemisinins. Postgrad Med J **81:**71-8.

174. **Woodrow, C. J., and S. Krishna.** 2006. Antimalarial drugs: recent advances in molecular determinants of resistance and their clinical significance. Cell Mol Life Sci **63:**1586-96.

175. **Xi, G., R. G. Leke, L. W. Thuita, A. Zhou, R. J. Leke, R. Mbu, and D. W. Taylor.** 2003. Congenital exposure to Plasmodium falciparum antigens: prevalence

and antigenic specificity of in utero-produced antimalarial immunoglobulin M antibodies. Infect Immun **71:**1242-6.

176. **Yayon, A., Z. I. Cabantchik, and H. Ginsburg.** 1984. Identification of the acidic compartment of Plasmodium falciparum-infected human erythrocytes as the target of the antimalarial drug chloroquine. Embo J **3:**2695-700.

177. **Yeates, C.** 2003. DB-289 Immtech International. IDrugs **6:**1086-93.

178. **Yeramian, P., S. R. Meshnick, S. Krudsood, K. Chalermrut, U. Silachamroon, N. Tangpukdee, J. Allen, R. Brun, J. J. Kwiek, R. Tidwell, and S. Looareesuwan.** 2005. Efficacy of DB289 in Thai patients with Plasmodium vivax or acute, uncomplicated Plasmodium falciparum infections. J Infect Dis **192:**319-22.

179. **Zhao, M., L. Ratmeyer, R. G. Peloquin, S. Yao, A. Kumar, J. Spychala, D. W. Boykin, and W. D. Wilson.** 1995. Small changes in cationic substituents of diphenylfuran derivatives have major effects on the binding affinity and the binding mode with RNA helical duplexes. Bioorg Med Chem **3:**785-94.

180. **Zhou, L., K. Lee, D. R. Thakker, D. W. Boykin, R. R. Tidwell, and J. E. Hall.** 2002. Enhanced permeability of the antimicrobial agent 2,5-bis(4-amidinophenyl)furan across Caco-2 cell monolayers via its methylamidoidme prodrug. Pharm Res **19:**1689-95.

181. **Zhou, L., D. R. Thakker, R. D. Voyksner, M. Anbazhagan, D. W. Boykin, J. E. Hall, and R. R. Tidwell.** 2004. Metabolites of an orally active antimicrobial prodrug, 2,5-bis(4-amidinophenyl)furan-bis-O-methylamidoxime, identified by liquid chromatography/tandem mass spectrometry. J Mass Spectrom **39:**351-60.

182. **Zhou, L., R. D. Voyksner, D. R. Thakker, C. E. Stephens, M. Anbazhagan, D. W. Boykin, J. E. Hall, and R. R. Tidwell.** 2002. Characterizing the fragmentation of 2,5-bis (4-amidinophenyl)furan-bis-O-methylamidoxime and selected metabolites using ion trap mass spectrometry. Rapid Commun Mass Spectrom **16:**1078-85.